



High-resolution X-ray tomography

Rajmund Mokso

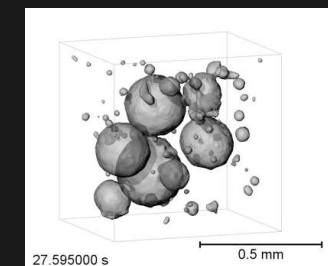
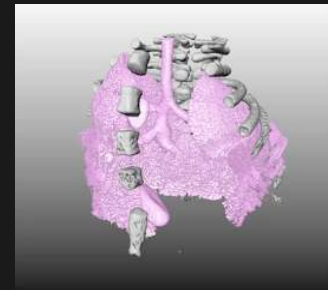
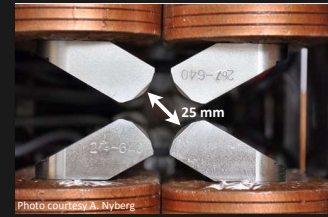
Solid Mechanics & Max IV Laboratory, Lund University

Outline

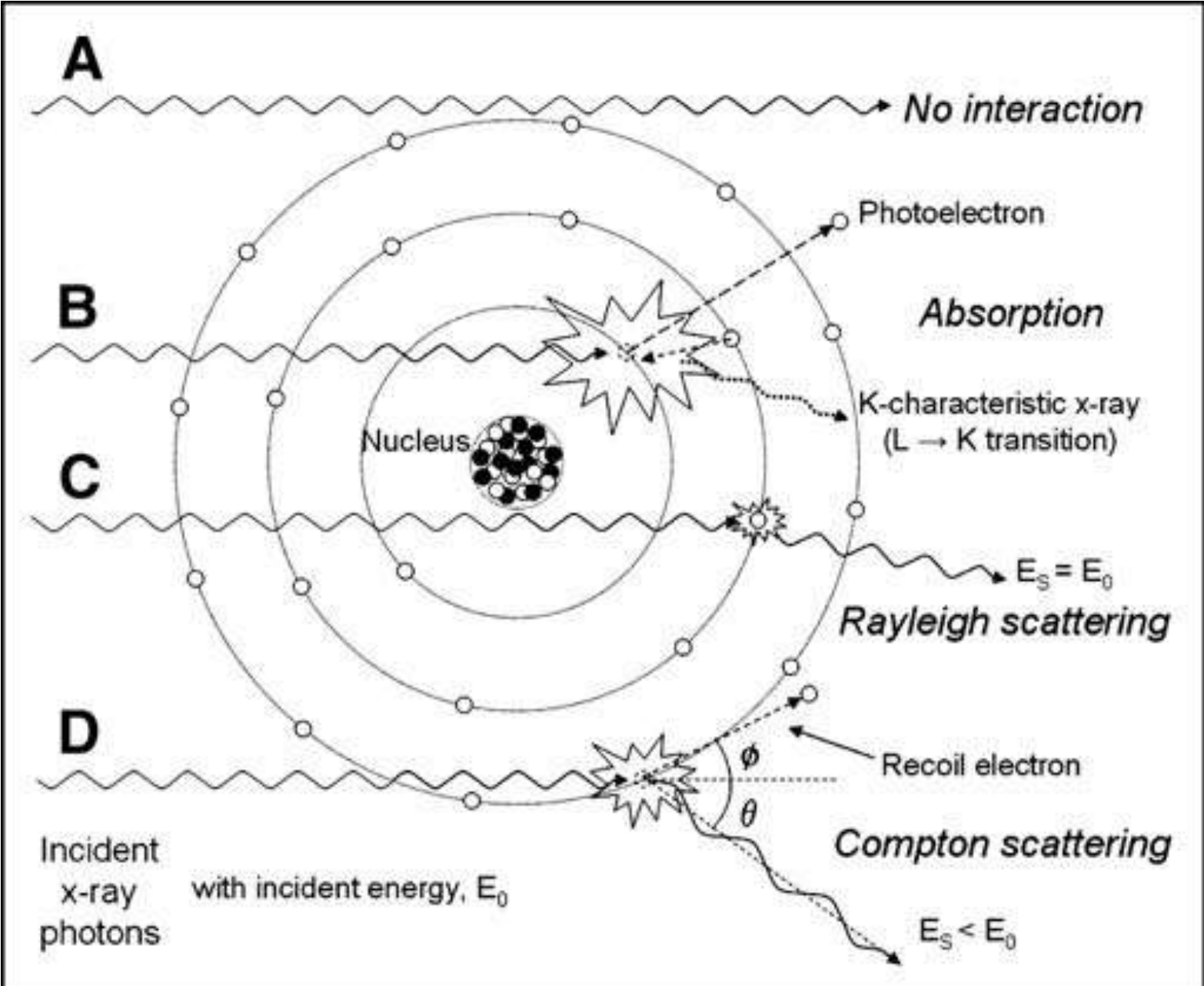
- I. Brief introduction into tomographic microscopy
 - I. Acquisition and reconstruction

- II. Applications
 - I. Bio: lungs
 - II. Hard matter: Aluminum foams

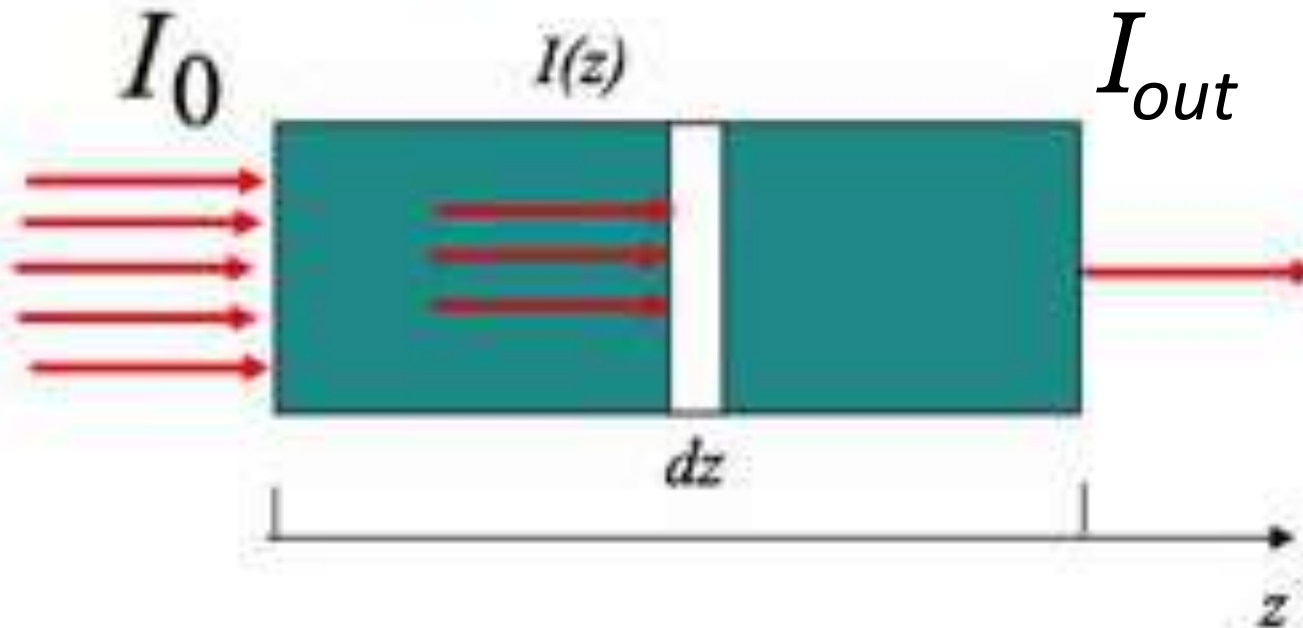
- III. Overview of MAX IV instruments for imaging
 - I. Beamlines, techniques



Absorption and scattering



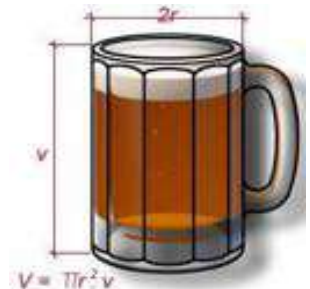
X-ray attenuation in the object



$$-dI = \mu \cdot I(z) dz \Rightarrow I(z) = I_0 \cdot e^{-\mu z}$$

μ^{-1} - the absorption length

Beer-Lambert law

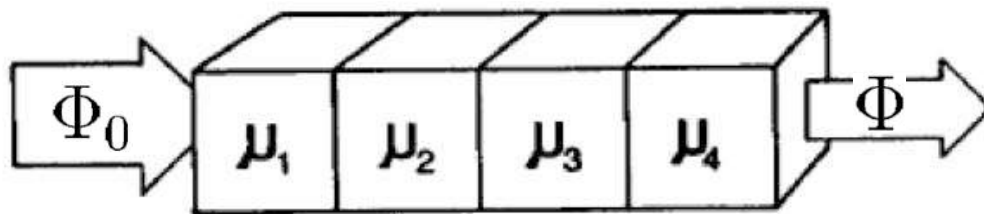


polychromatic case

$$\Phi = \int_E \Phi_0(E) e^{-\int_{SD} \mu(l,E) dl} dE$$

monochromatic case

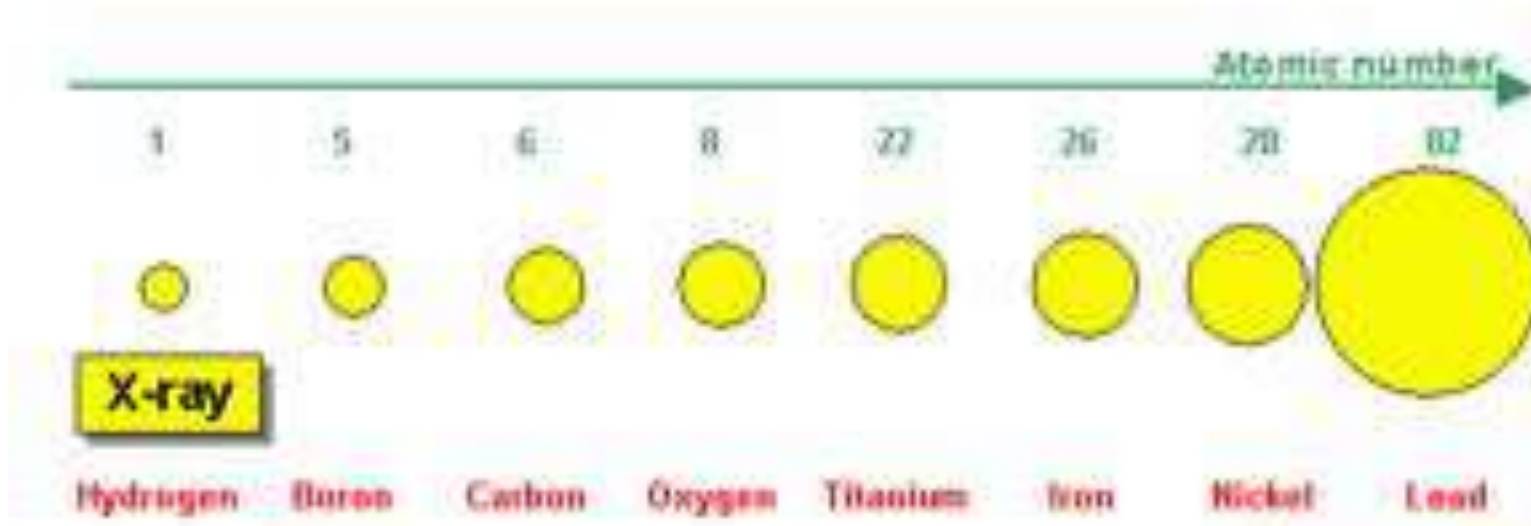
$$\Phi = \Phi_0(E) e^{-\int_{SD} \mu(l,E) dl}$$



The attenuation is linear and additive
(this is why tomography works!)

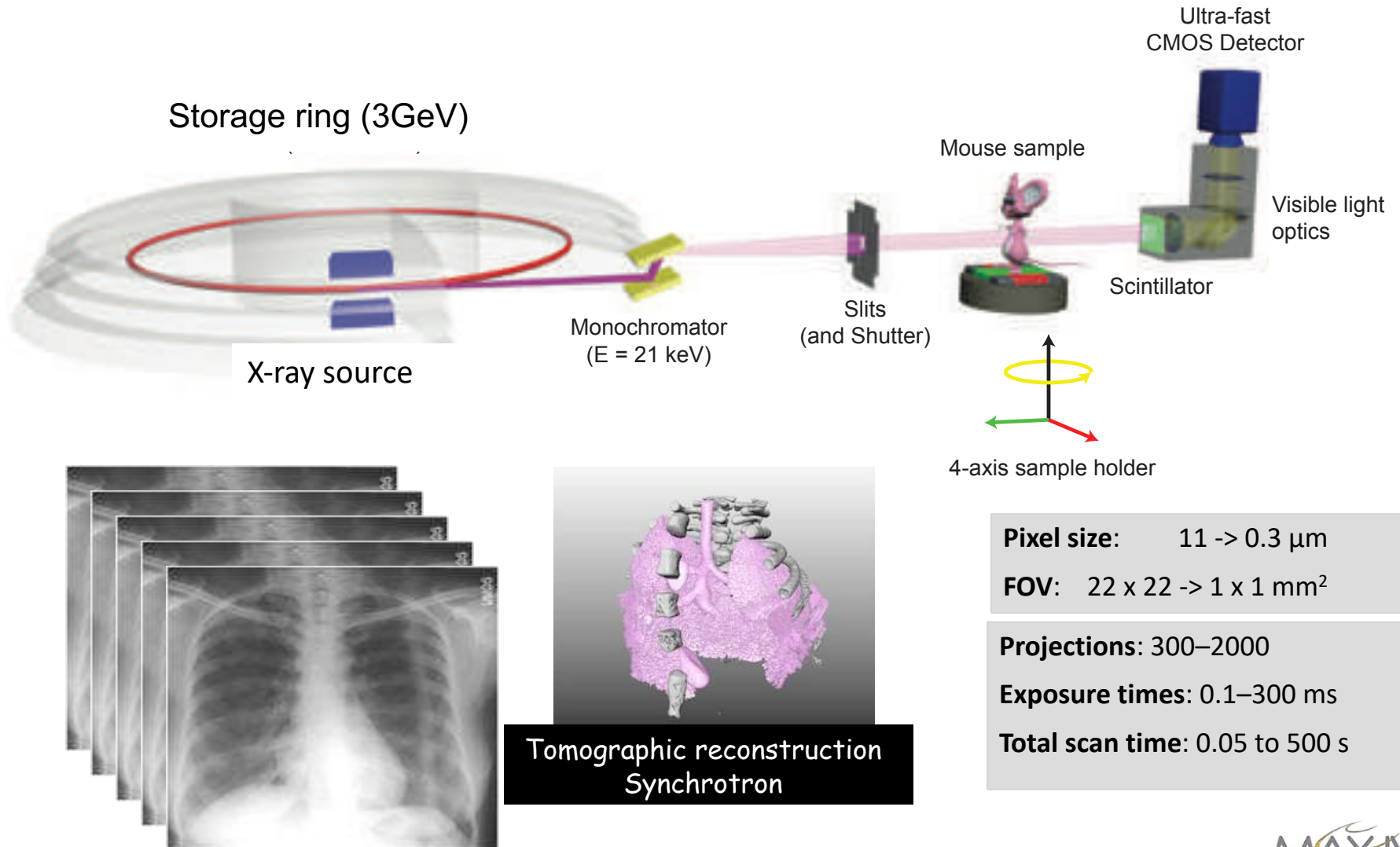


Probing matter with X-rays



$$\text{X-rays} \quad \sigma_{abs} \propto Z^4 \cdot (\hbar\omega)^{-3}$$

What is imaging?



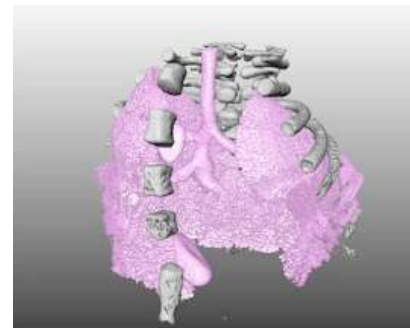
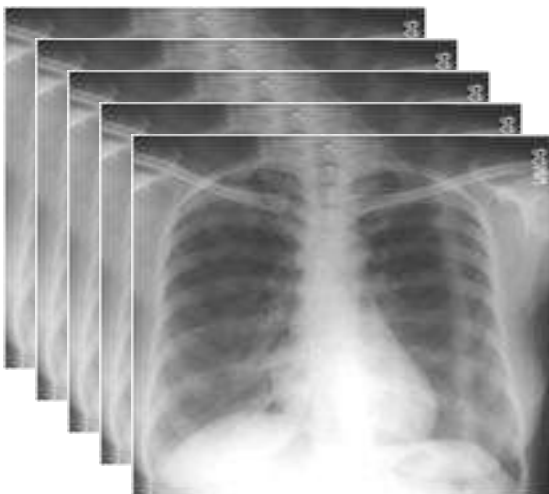
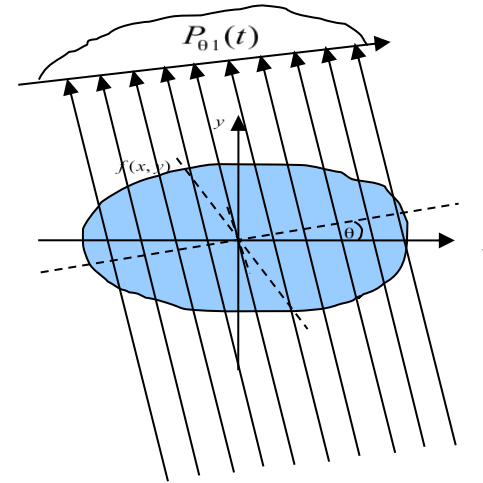
Tomographic reconstruction concepts?

Numerical (algebraic)

$$Ax = b$$

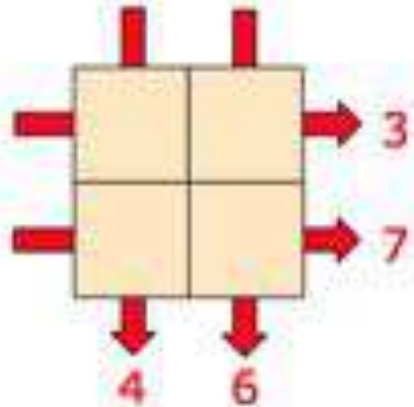
| | | | | |
|----------------|----------------|----------------|----------------|----------------|
| $x_1 = x_{11}$ | $x_2 = x_{12}$ | $x_3 = x_{13}$ | $x_4 = x_{14}$ | $x_5 = x_{15}$ |
| $x_2 = x_{21}$ | $x_1 = x_{22}$ | $x_3 = x_{23}$ | $x_4 = x_{24}$ | $x_5 = x_{25}$ |
| $x_3 = x_{31}$ | $x_2 = x_{32}$ | $x_1 = x_{33}$ | $x_4 = x_{34}$ | $x_5 = x_{35}$ |
| $x_4 = x_{41}$ | $x_3 = x_{42}$ | $x_2 = x_{43}$ | $x_1 = x_{44}$ | $x_5 = x_{45}$ |
| $x_5 = x_{51}$ | $x_4 = x_{52}$ | $x_3 = x_{53}$ | $x_2 = x_{54}$ | $x_1 = x_{55}$ |

Analytical (backprojection)



Tomographic reconstruction
Synchrotron

Analogy: the "Sudoku" Problem – 数独



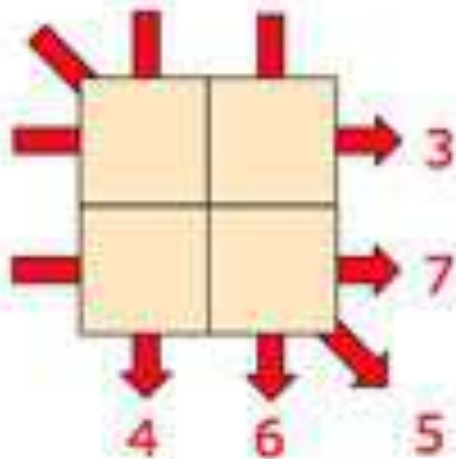
$$\begin{pmatrix} 1 & 0 & 1 & 0 \\ 0 & 1 & 0 & 1 \\ 1 & 1 & 0 & 0 \\ 0 & 0 & 1 & 1 \end{pmatrix} \begin{pmatrix} x_1 \\ x_2 \\ x_3 \\ x_4 \end{pmatrix} = \begin{pmatrix} 3 \\ 7 \\ 4 \\ 6 \end{pmatrix}$$

| | |
|---|---|
| 0 | 3 |
| 4 | 3 |

| | |
|---|---|
| 1 | 2 |
| | |

With enough rays, the problem has a unique solution.

Here, one more ray is enough to ensure a full-rank matrix:



$$\begin{pmatrix} 1 & 0 & 1 & 0 \\ 0 & 1 & 0 & 1 \\ 1 & 1 & 0 & 0 \\ 0 & 0 & 1 & 1 \\ 1 & 0 & 0 & 1 \end{pmatrix} \begin{pmatrix} x_1 \\ x_2 \\ x_3 \\ x_4 \end{pmatrix} = \begin{pmatrix} 3 \\ 7 \\ 4 \\ 6 \\ 5 \end{pmatrix}$$

The solution is now unique but it is still sensitive to the noise in the data.

Tomography

Damping of i -th X-ray through domain:

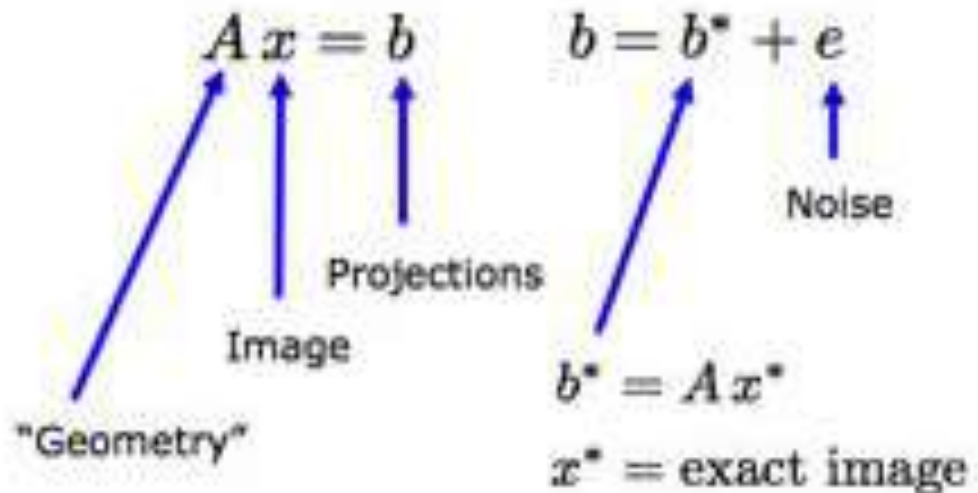
$$b_i = \int_{\text{ray}_i} \chi(\mathbf{s}) d\ell, \quad \chi(\mathbf{s}) = \text{attenuation coef.}$$

Assume $\chi(\mathbf{s})$ is a constant x_j in pixel j , leading to:

$$b_i = \sum_j a_{ij} x_j, \quad a_{ij} = \text{length of ray } i \text{ in pixel } j.$$

| | | | | |
|----------------|----------------|----------------|----------------|----------------|
| $x_1 = x_{11}$ | $x_2 = x_{12}$ | $x_3 = x_{13}$ | $x_4 = x_{14}$ | $x_5 = x_{15}$ |
| $x_2 = x_{21}$ | $x_3 = x_{22}$ | $x_4 = x_{23}$ | $x_5 = x_{24}$ | $x_6 = x_{25}$ |
| $x_3 = x_{31}$ | $x_4 = x_{32}$ | $x_5 = x_{33}$ | $x_6 = x_{34}$ | $x_7 = x_{35}$ |
| $x_4 = x_{41}$ | $x_5 = x_{42}$ | $x_6 = x_{43}$ | $x_7 = x_{44}$ | $x_8 = x_{45}$ |
| $x_5 = x_{51}$ | $x_6 = x_{52}$ | $x_7 = x_{53}$ | $x_8 = x_{54}$ | $x_9 = x_{55}$ |

This leads to a large linear system:

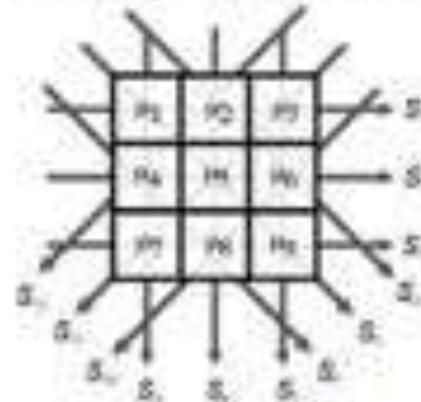
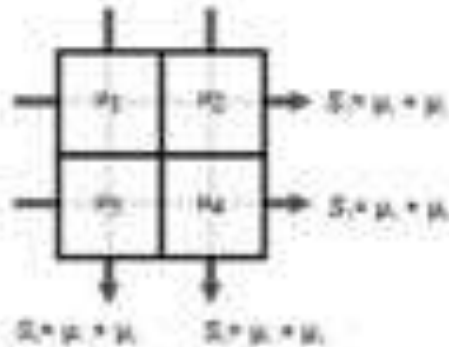


Tomography

- Direct inversion (solving N equations with N unknowns)



Godfrey Hounsfield



- Hounsfield in 1967 solved 28000 equations simultaneously!
- Need more than N^2 measurements to overcome linear independence



NOBELFÖRSAMLINGEN KAROLINSKA INSTITUTET
THE NOBEL ASSEMBLY AT THE KAROLINSKA INSTITUTE

11 October 1979

The Nobel Assembly of Karolinska Institutet has decided today to award the Nobel Prize in Physiology or Medicine for 1979 jointly to

Allan M Cormack and Godfrey Newbold Hounsfield

for the "development of computer assisted tomography".

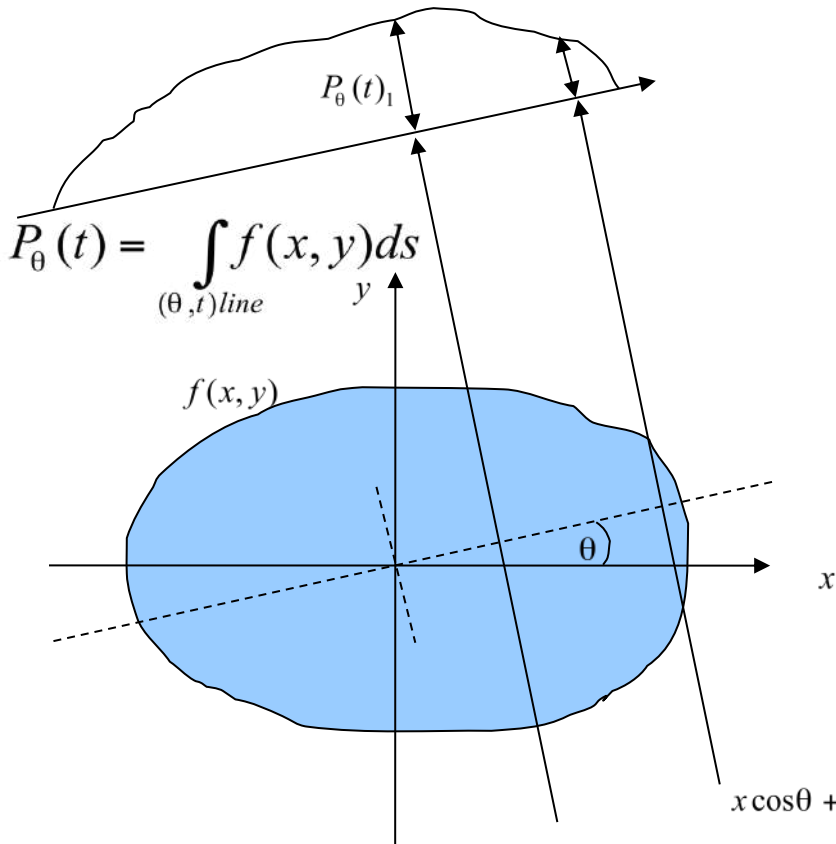
Tomography

Johan Radon, *Über die Bestimmung von Funktionen durch ihre Integralwerte Längs gewisser Mannigfaltigkeiten*, Berichte Sächsische Akademie der Wissenschaften, Leipzig, Math.-Phys. Kl., 69, pp. 262-277, 1917.

Main result: An object can be perfectly reconstructed from a full set of projections.



Tomography



Fourier transform of the projection

$$S_{\theta}(w) = \int_{-\infty}^{\infty} P_{\theta}(t) e^{-j2\pi wt} dt$$

2D Fourier transform of f(x,y):

$$F(u, v) = \int_{-\infty}^{\infty} \int_{-\infty}^{\infty} f(x, y) e^{-j2\pi(ux+vy)} dx dy$$

For simplicity v=0 (just a rotation)

$$F(u, 0) = \int_{-\infty}^{\infty} \int_{-\infty}^{\infty} f(x, y) e^{-j2\pi ux} dx dy$$

This allows to split the integral:

$$F(u, 0) = \int_{-\infty}^{\infty} \left[\int_{-\infty}^{\infty} f(x, y) dy \right] e^{-j2\pi ux} dx$$

$$P_{\theta=0}(x) = \int_{-\infty}^{\infty} f(x, y) dy$$

$$F(u, 0) = \int_{-\infty}^{\infty} P_{\theta=0}(x) e^{-j2\pi ux} dx$$

radon transform of f(x,y):

$$f(x, z) = \int_0^{\pi} \left[\int_{-\infty}^{\infty} S_{\theta}(w) |w| e^{i2\pi wt} dw \right] d\theta$$

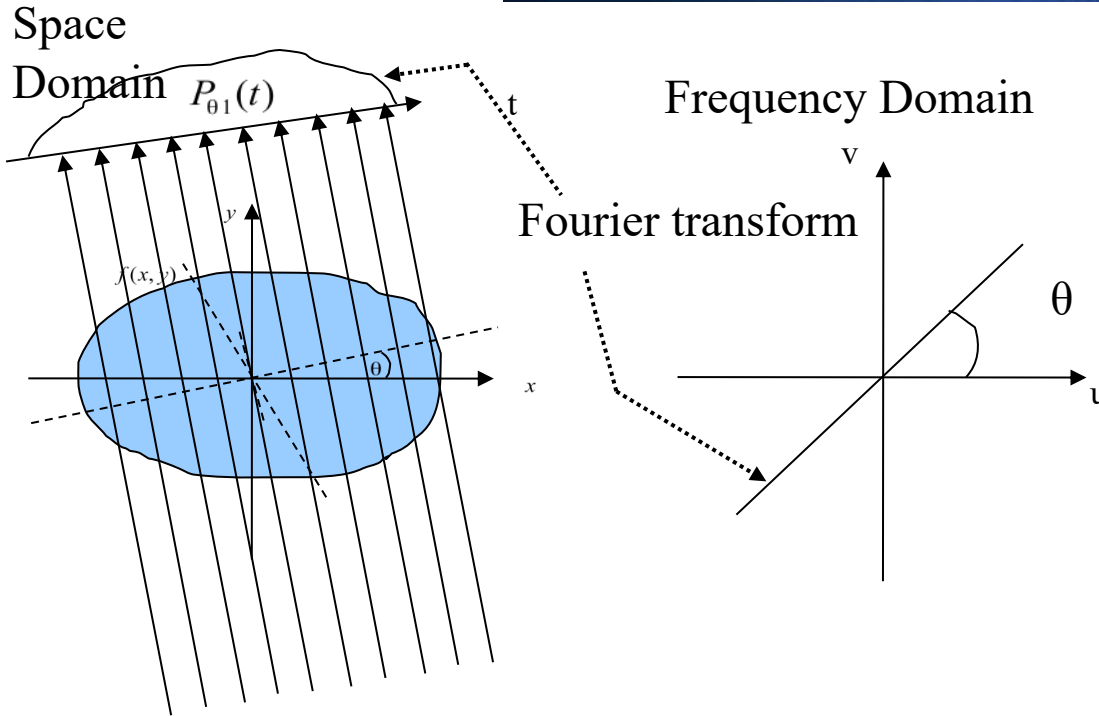
Determinant of Jacobian of the change from cartesian to polar coordinates

FOURIER SLICE THEOREM:

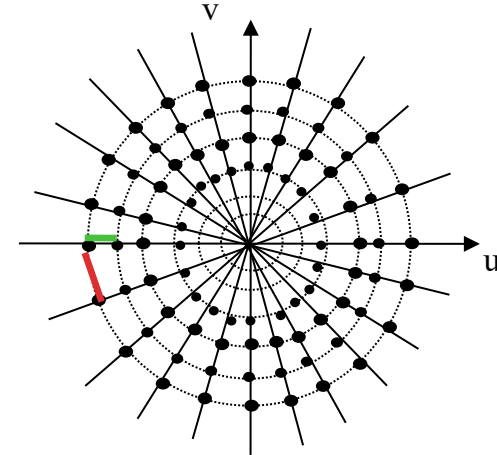
$F(u, 0) = S_{\theta=0}(u)$

The Fourier transform of the projection gives the value of the 2D Fourier transform of the object function along a line rotated by the tomographic angle.

Tomography



Collection of projections of an object at a number of angles



FILTERED BACKPROJECTION

For reconstruction we interpolate onto a square grid, but for high frequencies points are further apart, which results in image degradation

- Sum for each of the K angles between 0 and 180
- Measure the projection, $P_{\theta}(t)$ Fourier transform it to find $S_{\theta}(w)$
- Multiply it by the weighting function $2 \cdot \pi \cdot |w| / K$
- Sum over the image plane the inverse Fourier transforms of the filtered projections

$$\text{green line} = \frac{1}{\text{pixelSize} \times \text{CCDsize}}$$

$$\text{red line} = \frac{1}{2 \times \text{pixelSize}} \frac{\pi}{N_{proj}}$$

$$N_{proj} = \frac{\pi}{2} \cdot \text{CCDsize}$$

The classical approach to time-resolved tomography

Dynamic studies in 3D are possible if

the rate of structural changes in the sample $\{V_{\text{EVOL}}\} <$
spatial resolution $\{\delta R\}$ /scan time $\{t_{\text{SCAN}}\}$)

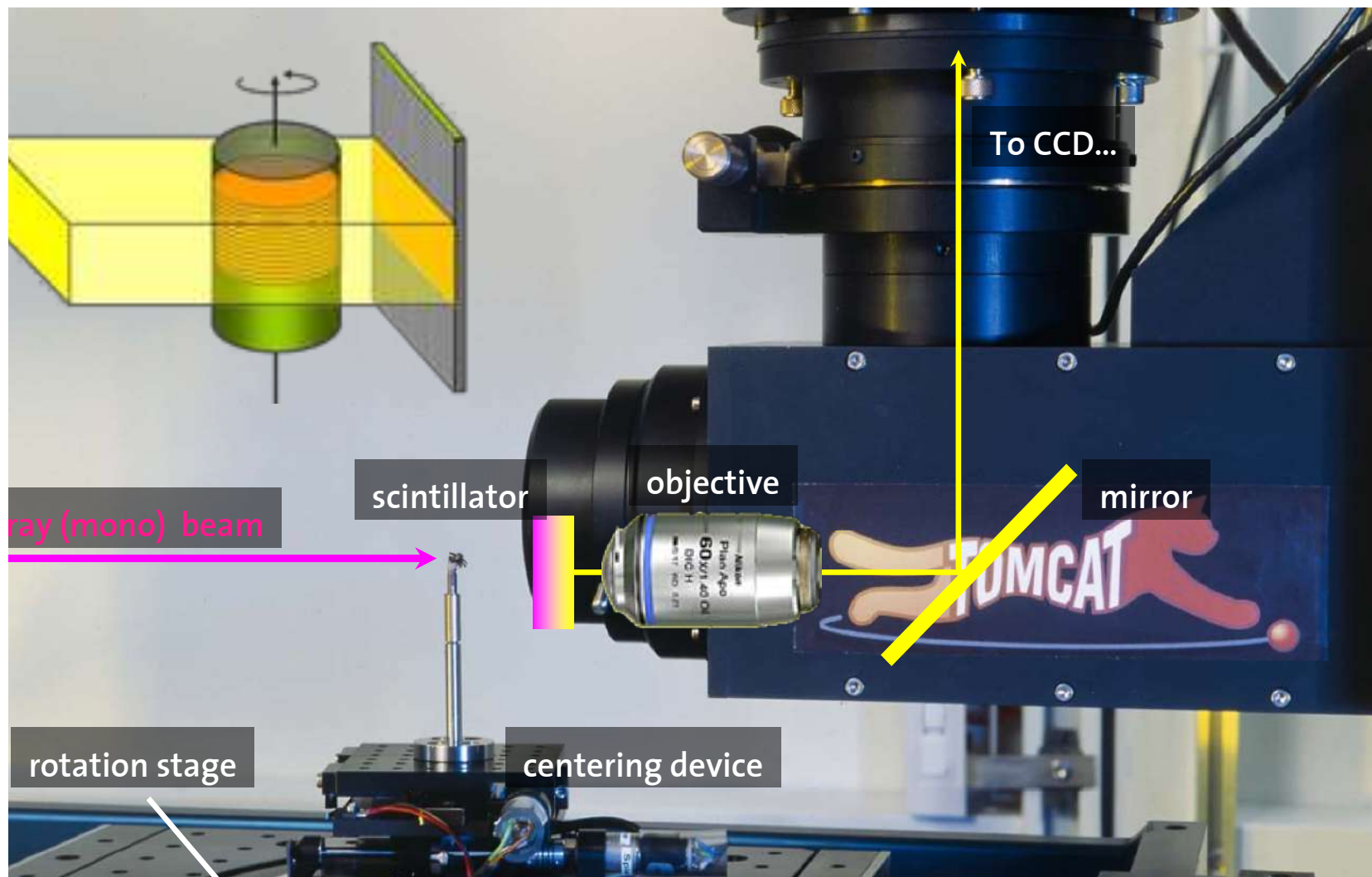
$$t_{\text{SCAN}} < \delta R / V_{\text{EVOL}}$$

0.5 s 5 μm 10 $\mu\text{m/s}$



Mokso et al, J/ Phys. D. 2013

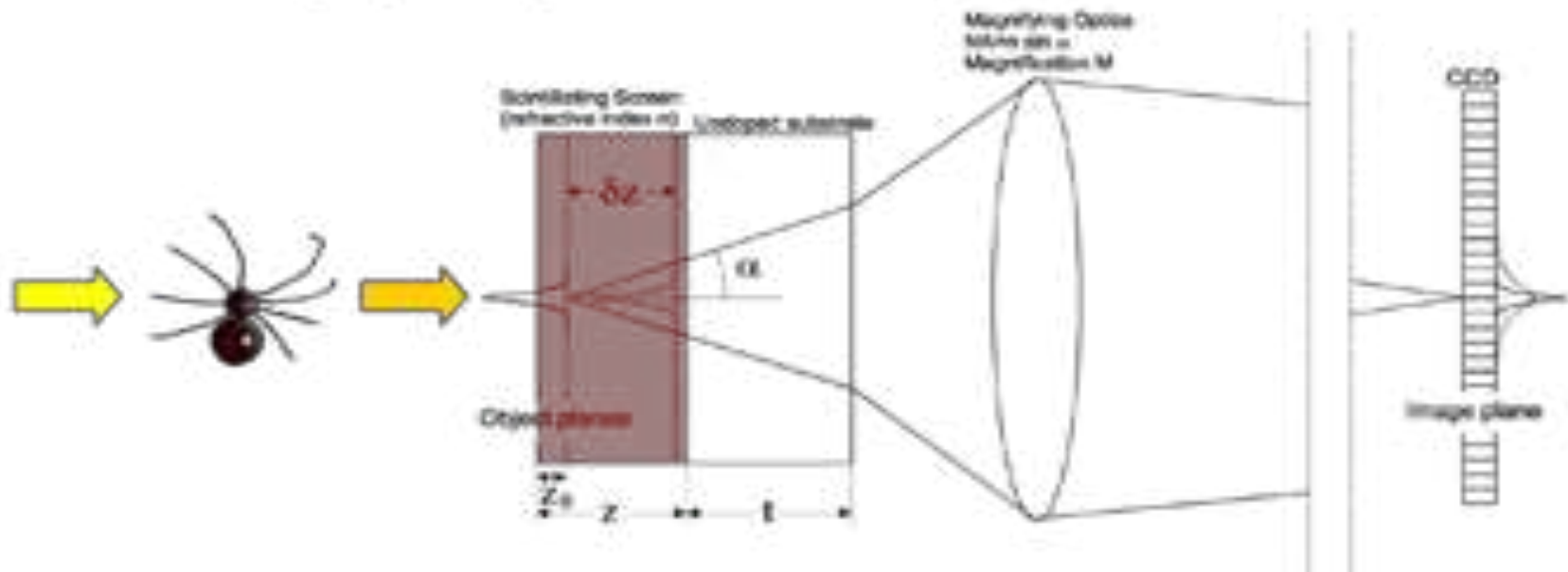
Indirect detectors



Indirect detectors

Indirect 2D X-ray detection

1. X-rays impinge on scintillating screen
2. Scintillator screen/thin powder converts X-rays to visible light
3. Visible light is collected by high efficiency lens
4. Lens magnify image onto CCD chip

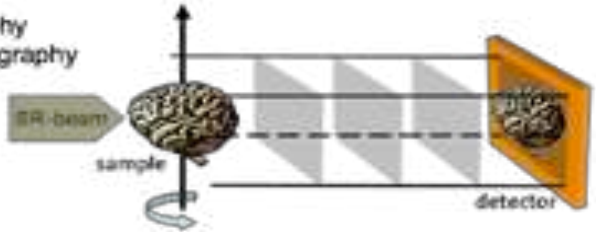


Imaging geometries

(i) Parallel beam microscopy

(i) Parallel beam microscopy

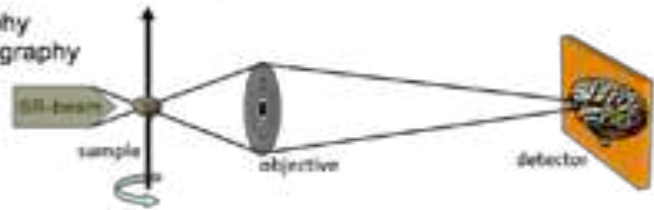
- Absorption Radiography / Tomography
- Phase contrast Radiography / Tomography
- Resolution ≥ 1 micron



(ii) TXM: Transmission (full-field) microscopy

(ii) TXM: Transmission (full field) microscopy

- Absorption Radiography / Tomography
- Phase contrast Radiography / Tomography
- High resolution, down to tens of nm
- Dose inefficient



(iii) SXM: Scanning microscopy

(iii) SXM: Scanning microscopy

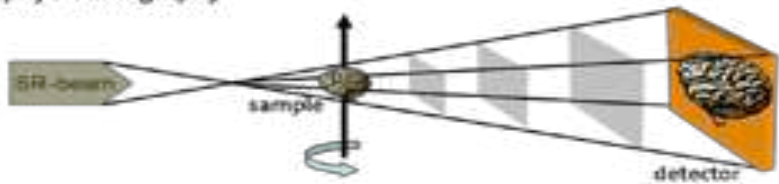
- Slow
- Chemical sensitivity / Phase contrast
- For coherent illumination geometry: CDI



(iv) PXM: Projection microscopy

(iv) PXM: Projection microscopy

- Phase contrast Radiography / Tomography
- Fast and dose efficient
- High resolution



The radiation dose

Absorbed dose:

$$D = \frac{E_{\text{abs}}}{m} = \frac{\Delta I h \nu}{V \rho} = \frac{(I_0 - I_1) h \nu}{\rho A \Delta x}$$

with

$$(I_0 - I_1) = I_0 \cdot \left[1 - e^{-\left(\frac{\mu_{\text{en}}}{\rho}\right) \rho \Delta x} \right]$$

Skin (entrance) dose:

$$D = N \cdot \left(\frac{\mu_{\text{en}}}{\rho} \right) h \nu,$$

E_{abs} : absorbed energy [J]

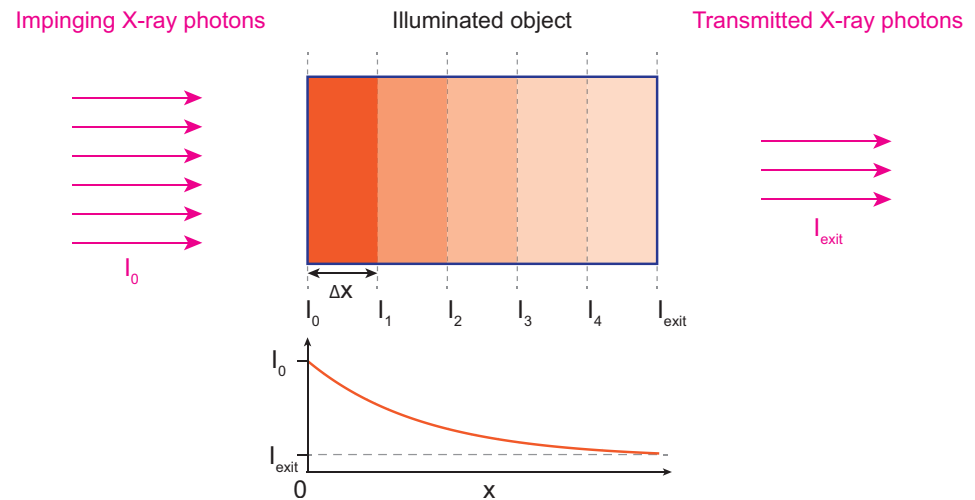
m : mass [kg]

ρ : density

ΔI : number of absorbed photons with energy $h\nu$

A : cross section area

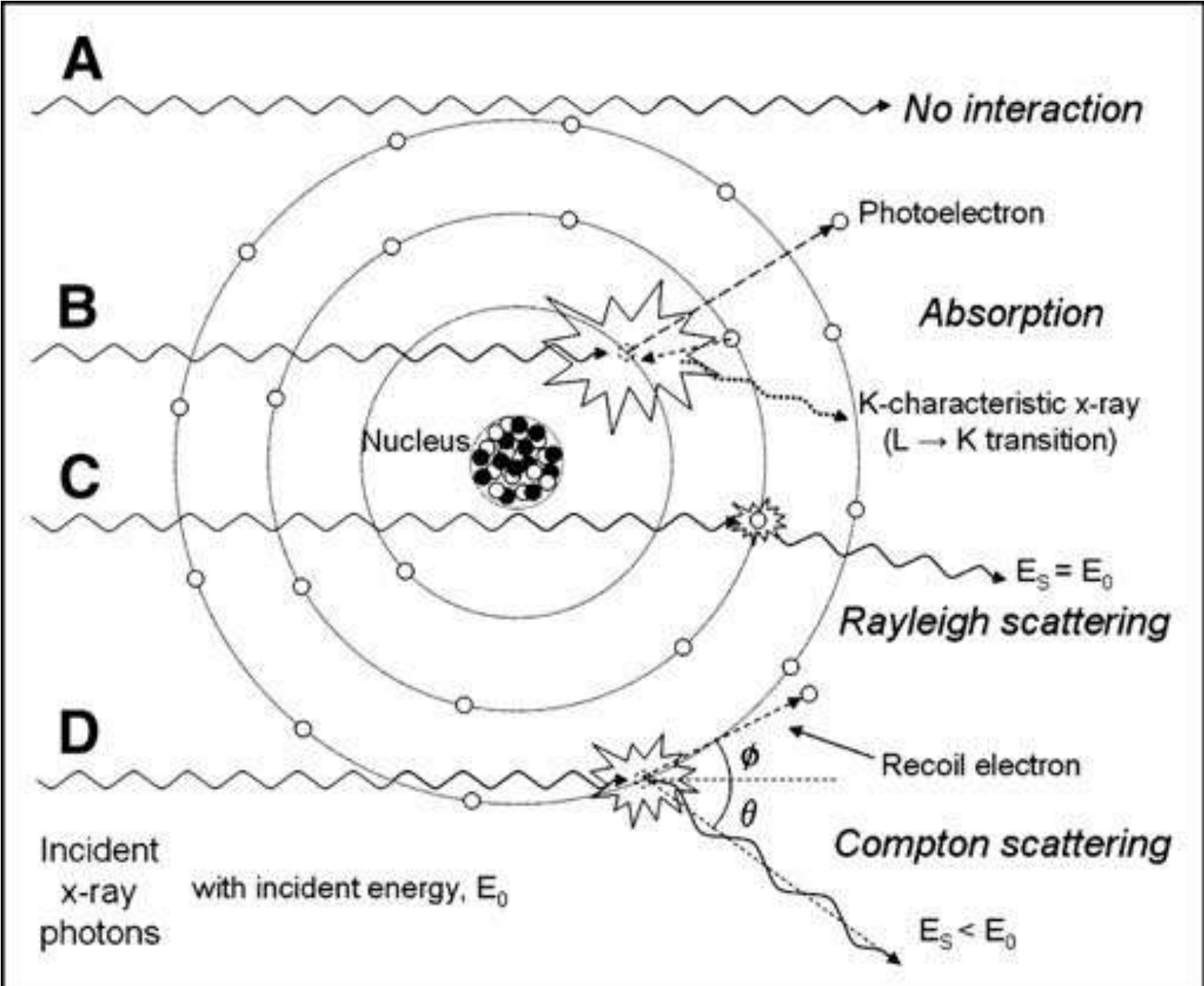
Δx : slice thickness



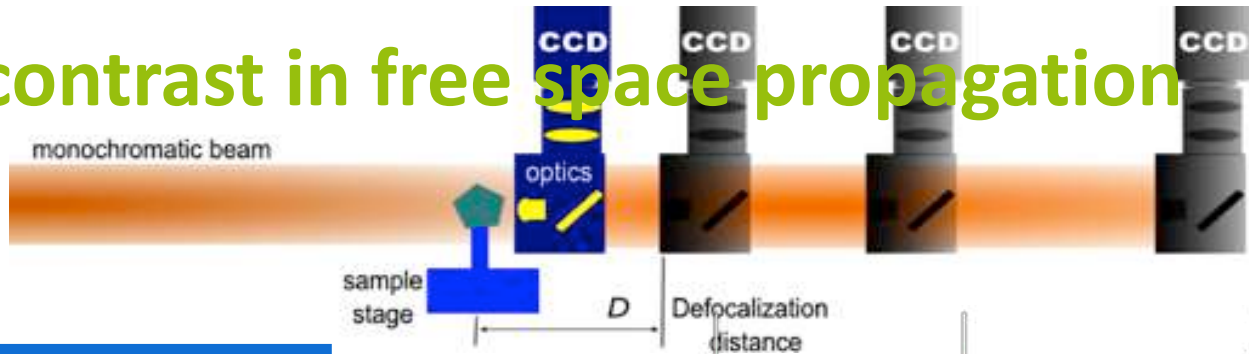
$$D [\text{Gy}] = \frac{I_0 h \nu}{\mu^{-1} \rho} \approx 1.602 \times 10^{-4} \cdot \frac{I_0 [\text{photons}/\mu\text{m}^2] \cdot h \nu [\text{eV}]}{\mu^{-1} [\mu\text{m}] \cdot \rho [\text{g}/\text{cm}^3]}.$$

[Howels et al.]

Absorption and scattering



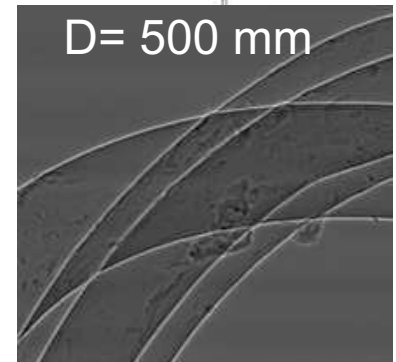
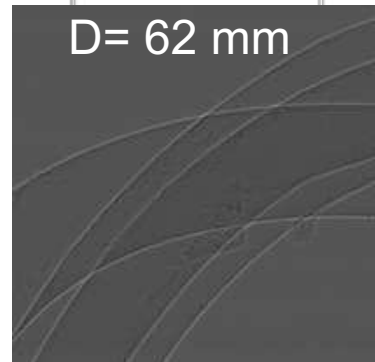
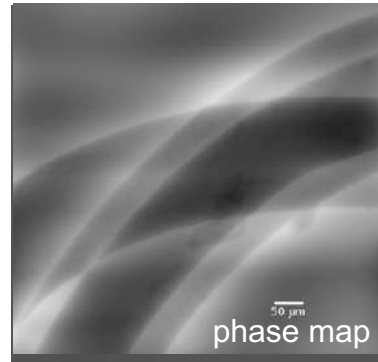
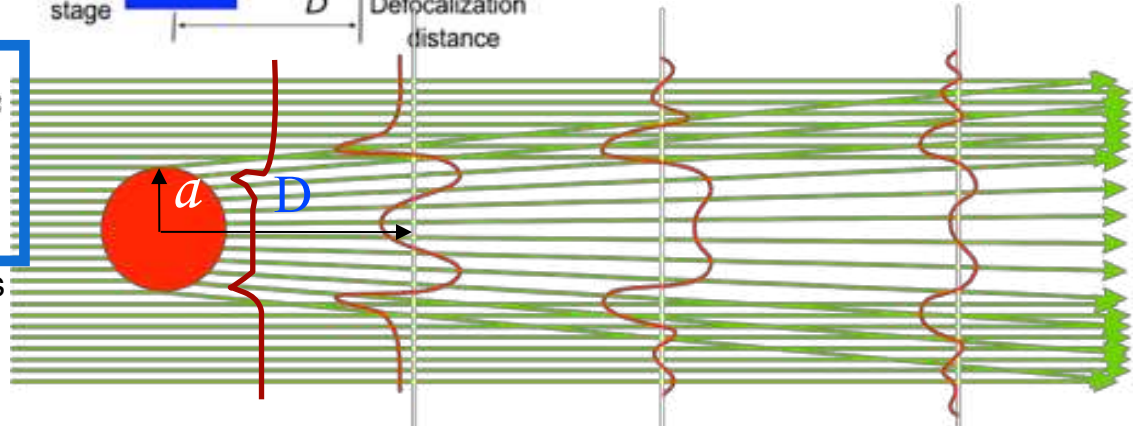
Phase contrast in free space propagation



$$U_D(x) = U_0(x) \otimes \sqrt{\frac{-i\pi}{\lambda \cdot D}} \cdot e^{\frac{i\pi}{\lambda \cdot D} \cdot x^2}$$

propagator

Born, M., and E. Wolf, 1990, Principles of Optics



Three phase fibers

Fresnel diffraction
Partially coherent illumination

$$\varphi(f) = \frac{\sum_m \sin(\pi \lambda D_m f^2) I_m(f)}{\sum_m 2 \sin^2(\pi \lambda D_m f^2)}$$

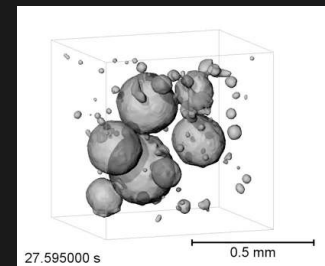
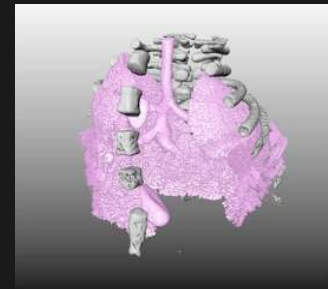
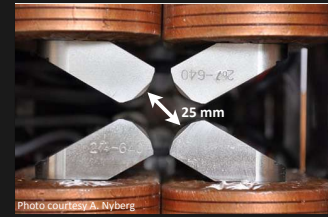
Cloetens et al. J. Phys. 1999

Outline

- I. Brief introduction into tomographic microscopy
 - I. Acquisition and reconstruction

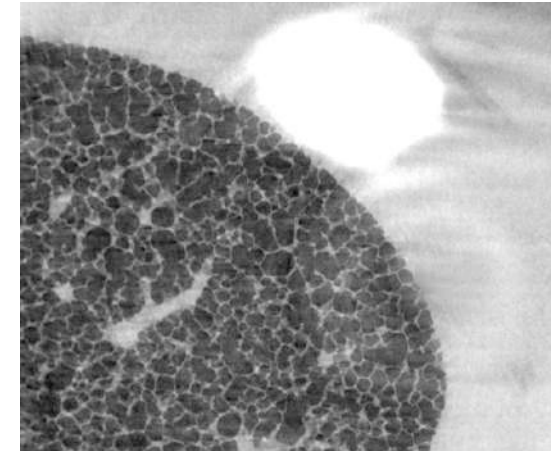
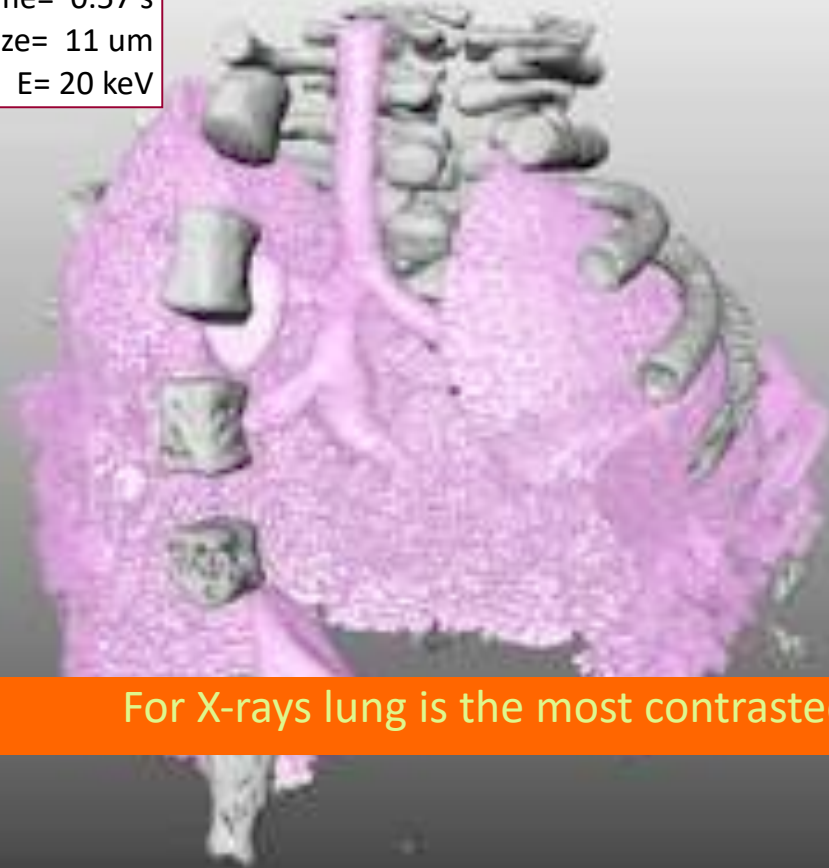
- II. Applications
 - I. Bio: lungs
 - II. Hard matter: Aluminum foams

- III. Overview of MAX IV instruments for imaging
 - I. Beamlines, techniques



exposure time= 1.1 ms
projections= 500
total scan time= 0.57 s
voxel size= 11 μm
E= 20 keV

3D lung imaging of lungs of a baby rat



For X-rays lung is the most contrasted 'soft' organ in the body

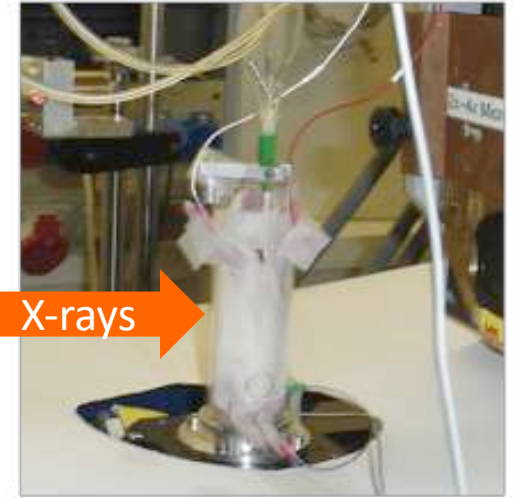
G. Lovric Phys Med 2016

R. Mokso et al AIP Conf. Proc. 1365 (2011)

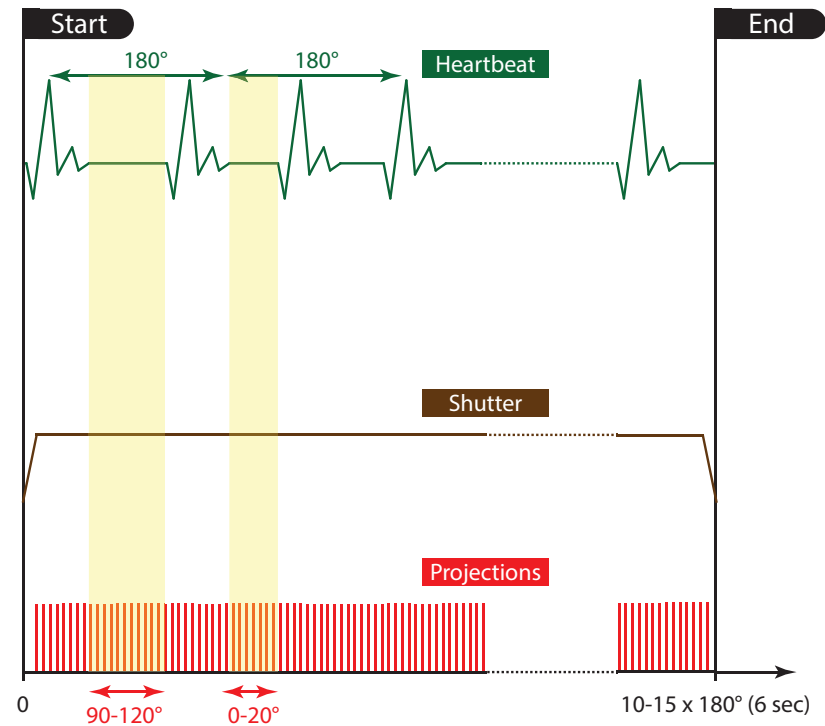
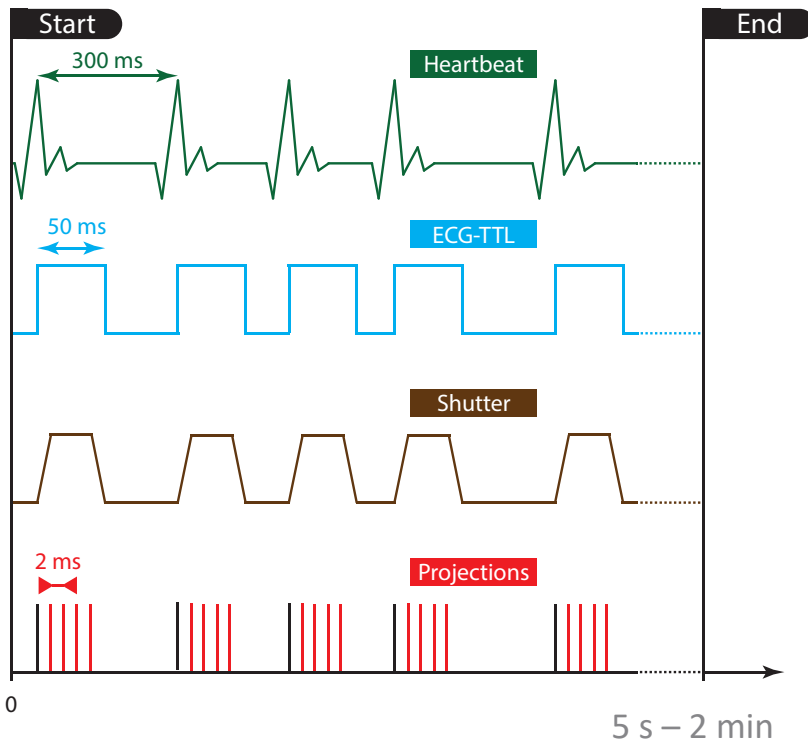
Gated acquisition mode

Ventilation and ECG

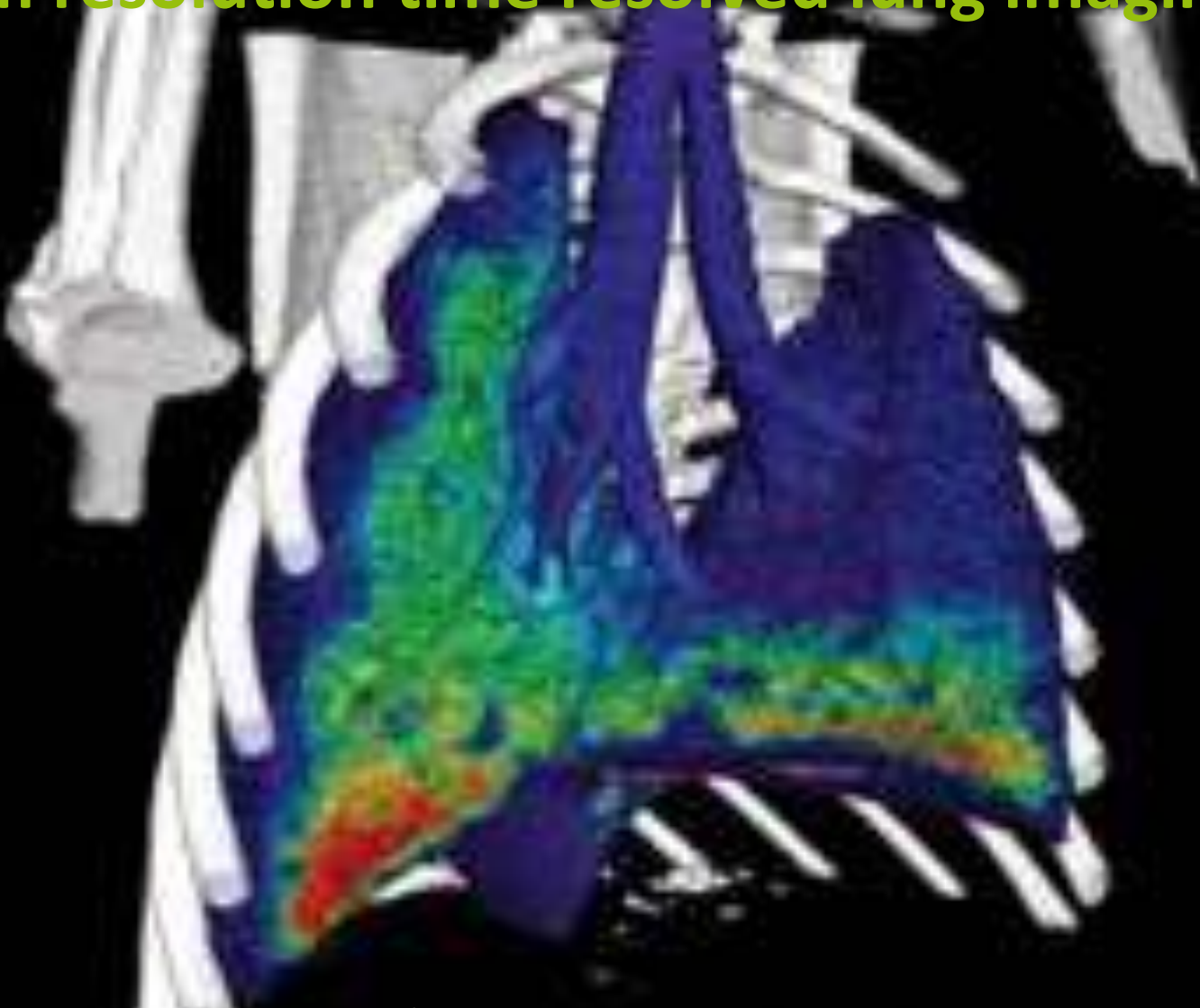
- Retrospective image guided gating



G. Lovric, PhD thesis



Medium resolution time resolved lung imaging

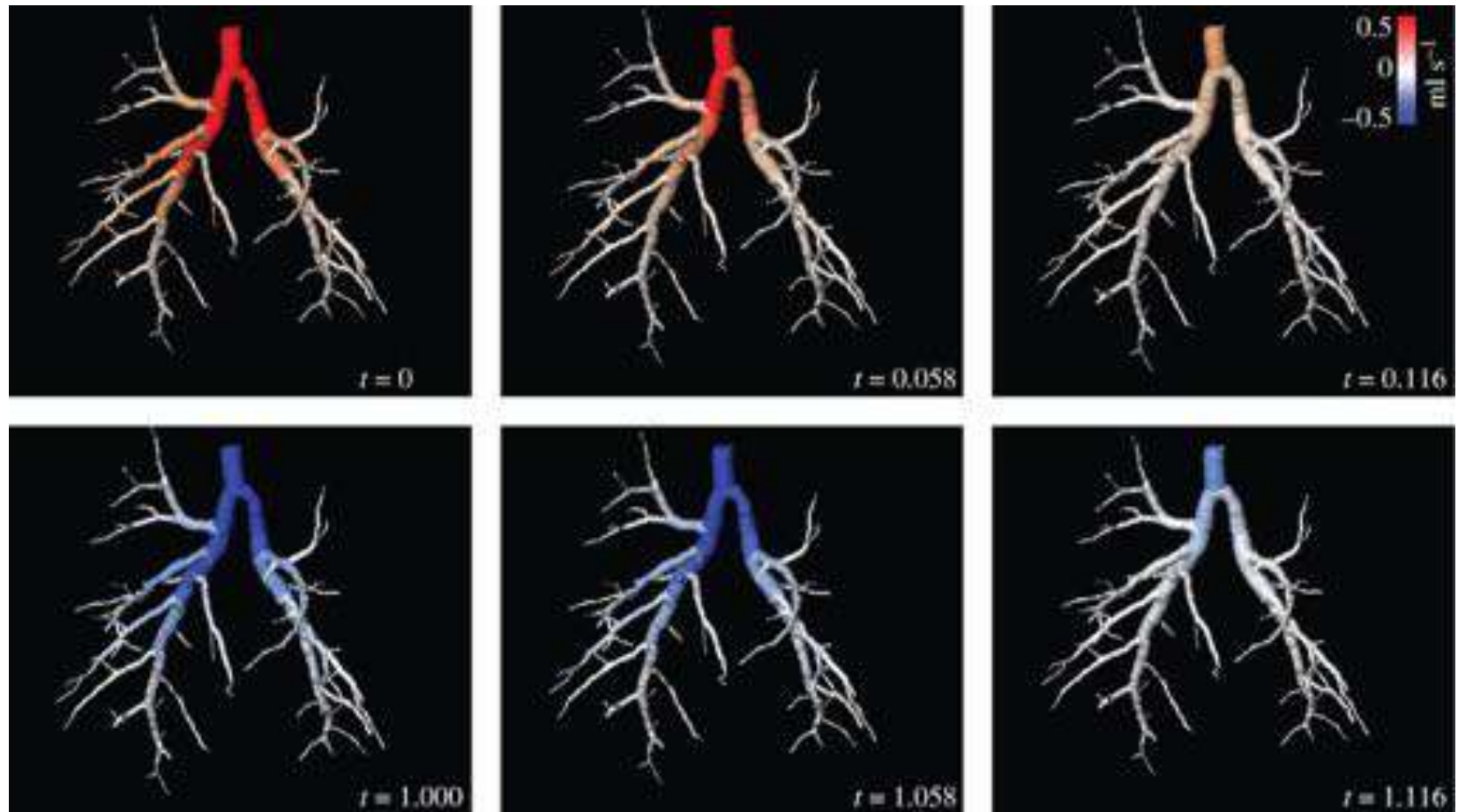


Three-dimensional representation of the total lung tissue displacement at the end-inspiration for a single time point (end-inspiration) of the four-dimensional dataset for mouse M1.

displacement (μm)



Distribution of air flow through an airway tree in rabbit lungs

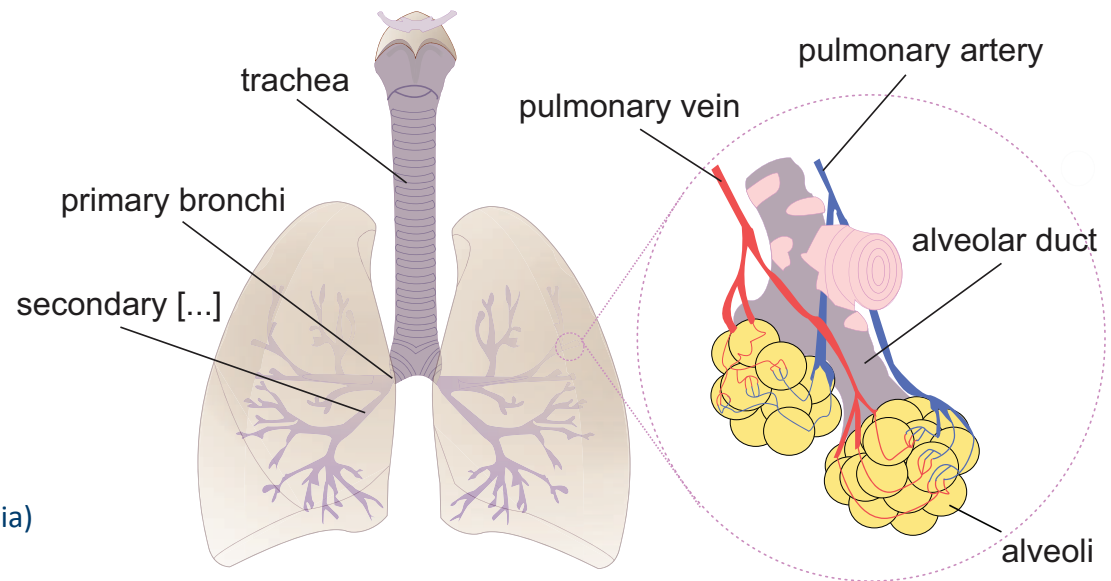


Stephen Dubsy et al. J. R. Soc. Interface 2012;9:2213-2224

Dynamic imaging of lungs: motivation

Ventilator-induced lung injury (VILI)

- Overextension of lung tissue in certain lung regions (mechanical damage, biotrauma)
- Still unclear how ventilation induces its deleterious effect [4]
- Hypothesis: local strains in the alveolar wall cause hotspots (overstretching regions)



Human lungs (Source: Wikipedia)

[4] Rausch, S. M. K., Haberthür, D., Stampanoni *et al.*, *Ann Biomed Eng* **39** (11), 2835 (2011).

The first insight into alveoli microstructure

A grayscale micro-CT scan of lung tissue showing the intricate, honeycomb-like structure of alveoli. The alveoli are small, rounded sacs that form a complex network. The image shows a cross-section of the lung, with the alveoli appearing as dark, interconnected clusters. The overall structure is highly porous and interconnected, typical of lung tissue.

Collaboration between Anders Larsson from Uppsala Uni. Hospital, SLS and ESRF.

1 mm

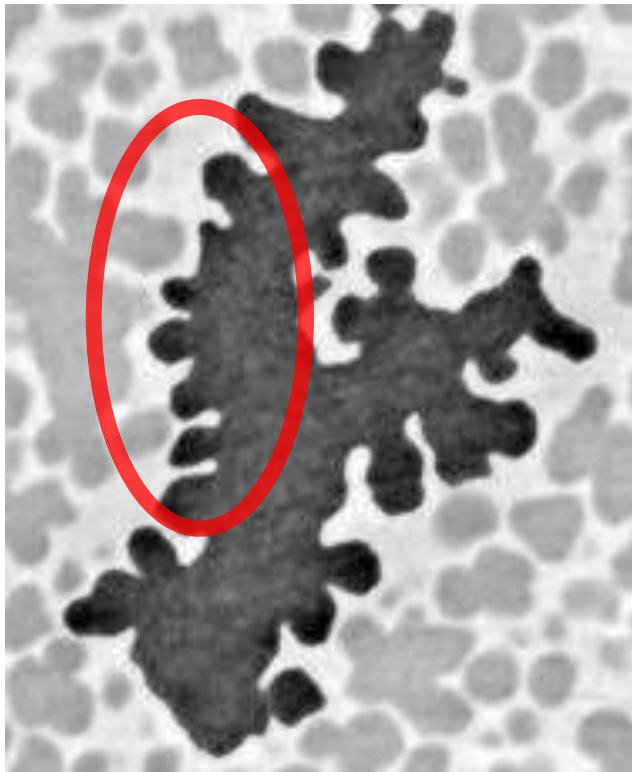
Lovric et al. Sci. Rep. 2017

Lung tissue quantification

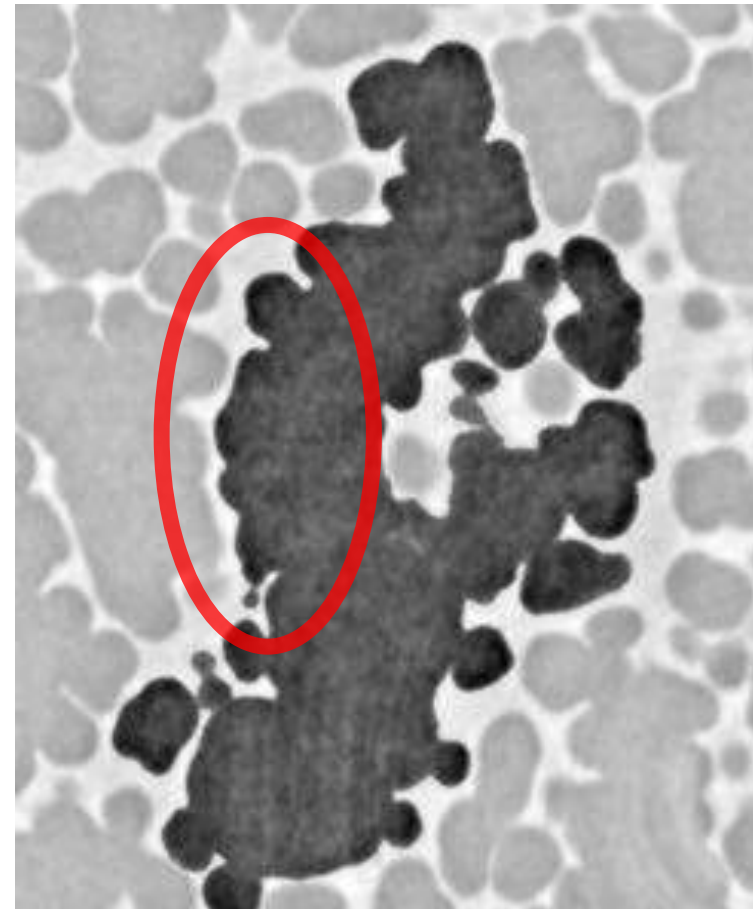
Challenges in lung tissue analysis

- How to detect non-linear and regional changes in the lung?
- How to quantify them?

G. Lovric, PhD thesis



$$\Delta p = 5 \text{ cmH}_2\text{O}$$

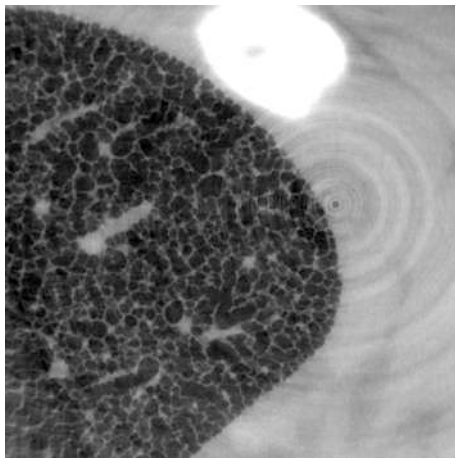


Alveoli dynamics quantification

A detailed insight into the lung

- Apply *quantification* and *labeling* tools, previously used for foam and bone data [14] and dendritic microstructures [15]

Original tomographic slice



1 mm

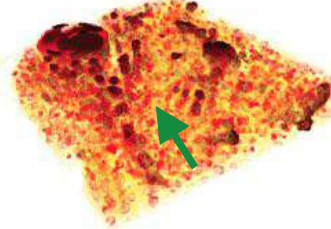
Thickness map



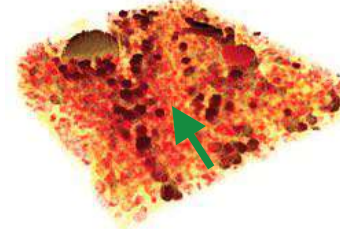
[3.5 x 3.5 x 0.6 mm³]

[3.5 x 3.5 x 0.6 mm³]

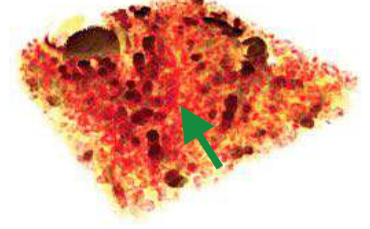
[3.5 x 3.5 x 0.6 mm³]



25 cmH₂O



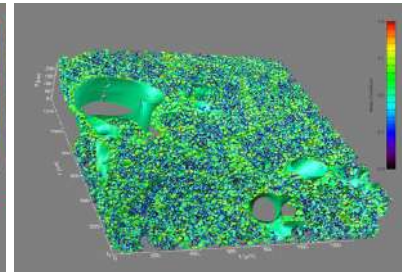
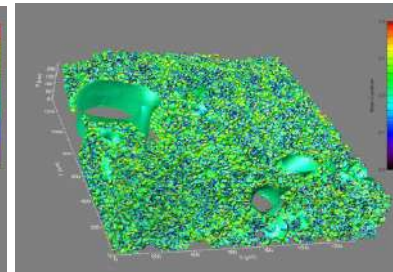
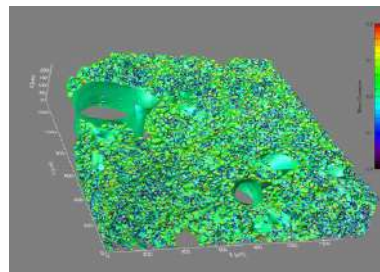
30 cmH₂O



35 cmH₂O



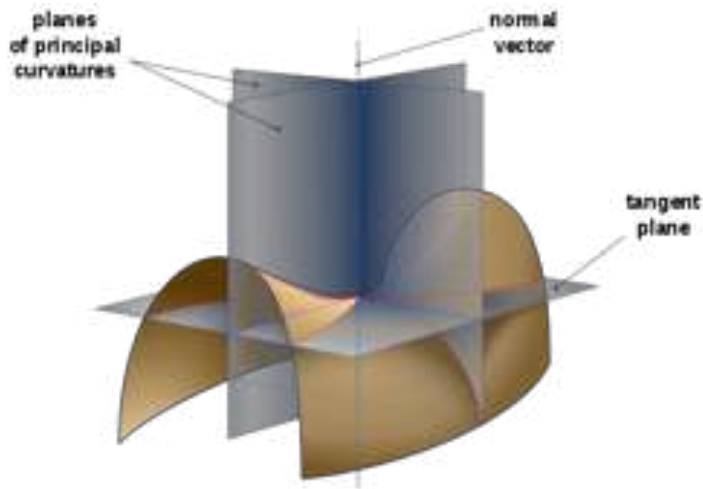
Curvature



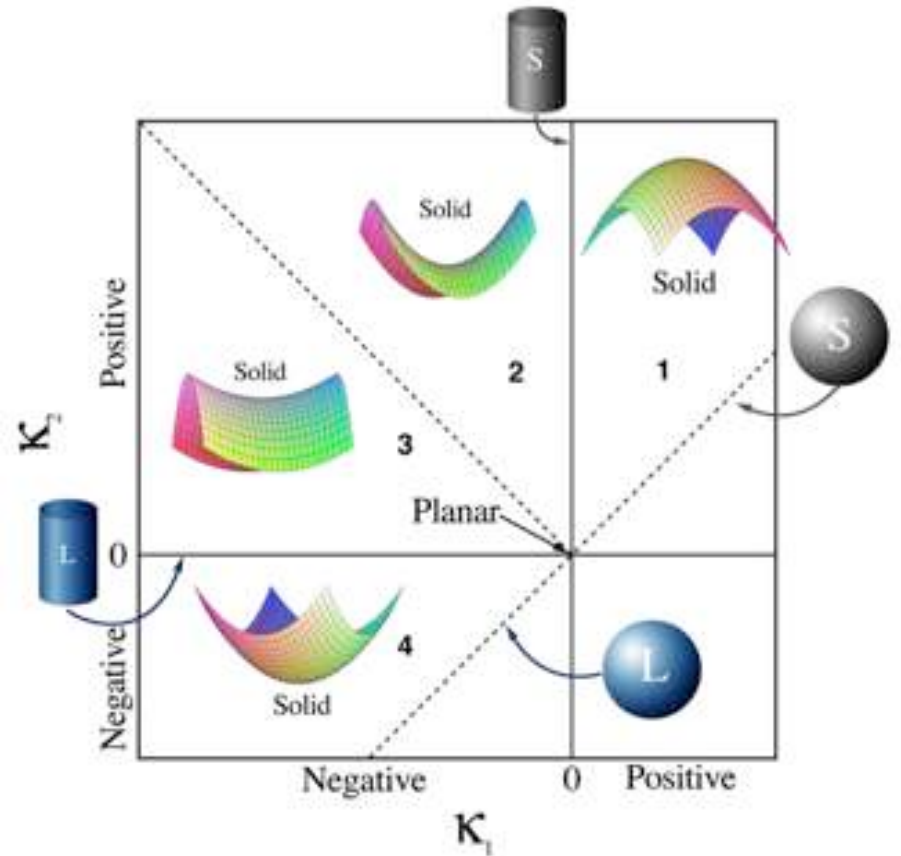
G. Lovric , PhD thesis, Lovric et al. in preparation



Curvature analysis

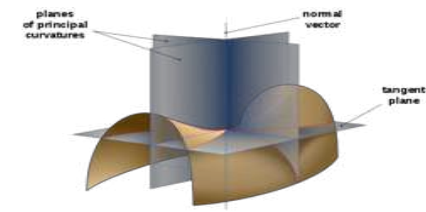


▲ Directions of principal curvatures
(Source: Wikipedia)

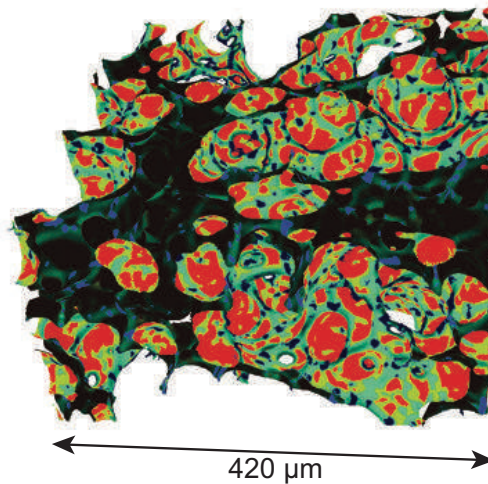


$\kappa_1, \kappa_2 \dots$ eigenvalues of the shape operator

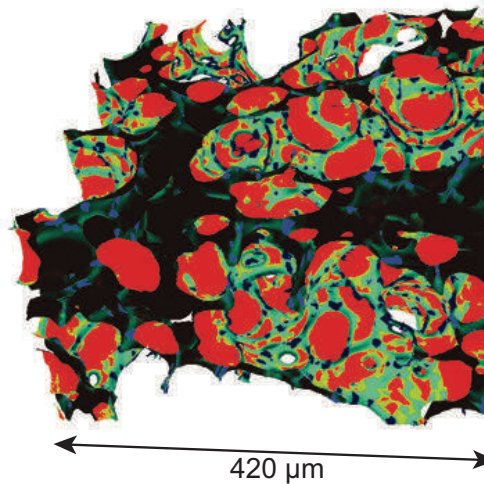
Shape analysis of lungs alveoli



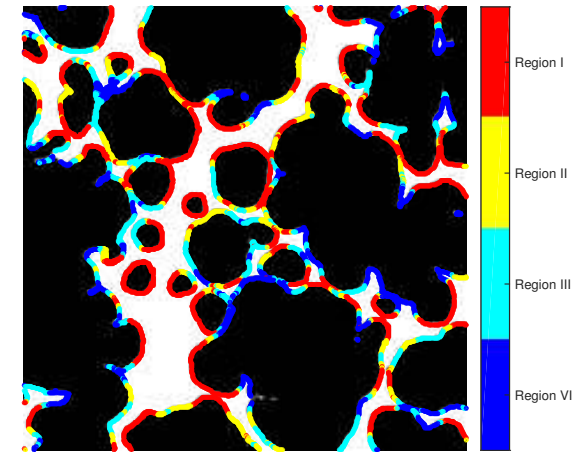
G. Lovric , PhD thesis



(a)



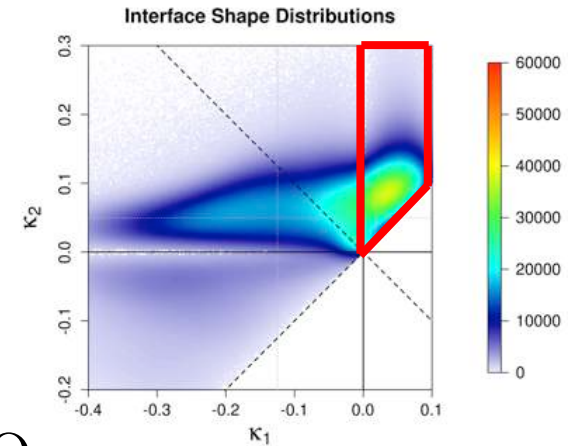
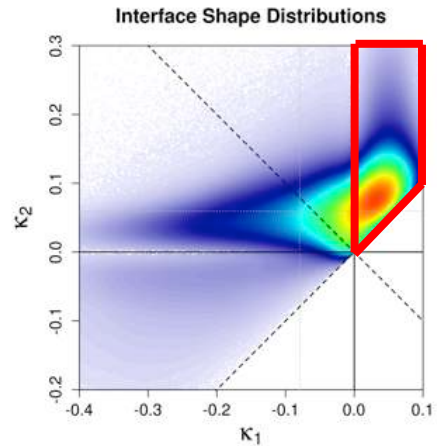
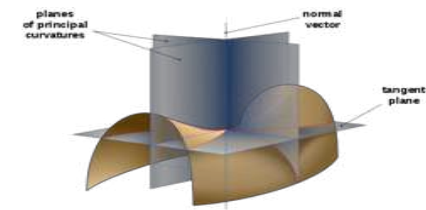
(b)



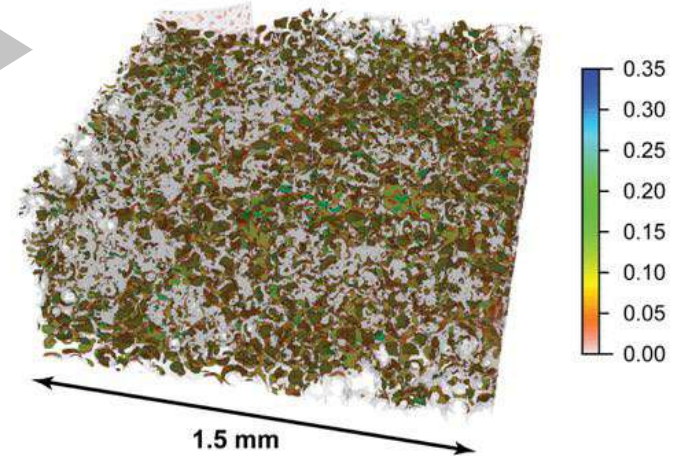
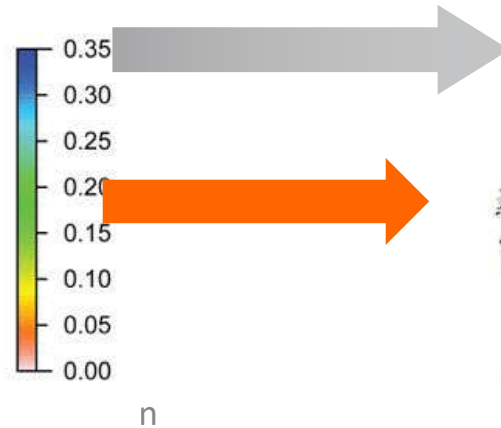
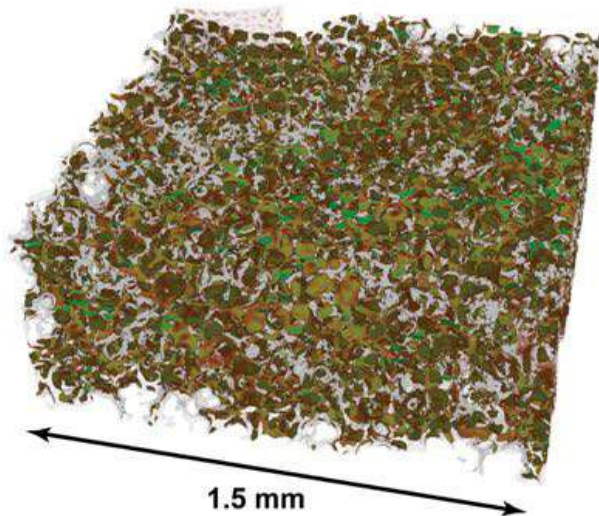
(c)

Figure 6.13. 3D visualization of the four regions from the ISD-plot with different geodesic radius: **(a)** depicts the calculation with radius $R = 3.5$ and **(b)** with $R = 15$. In **(c)** a 2D slice is shown from **(b)**.

Gated acquisition mode



$$\Delta p = 5 \text{ cmH}_2\text{O}$$

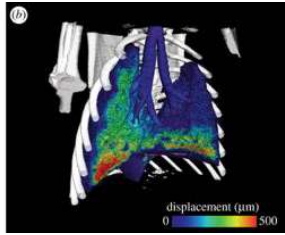


G. Lovric , PhD thesis, Lovric et al. in preparation

Hierarchical imaging of tissues

Medical imaging and therapy

(in vivo, medium resolution $>30\ \mu\text{m}$, low dose, large beam, large FOV)



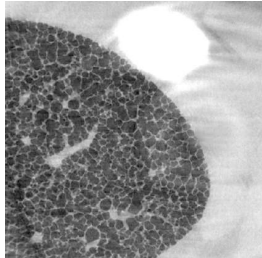
Longitudinal in vivo

The whole organ

2 mm

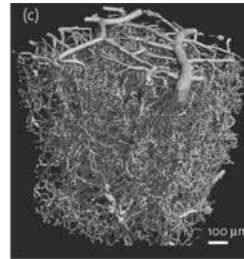


Down to a micrometer resolution
(rarely in vivo, high resolution $\sim 1\ \mu\text{m}$, higher dose, small FOV)



Accute in vivo

Zooming into organs

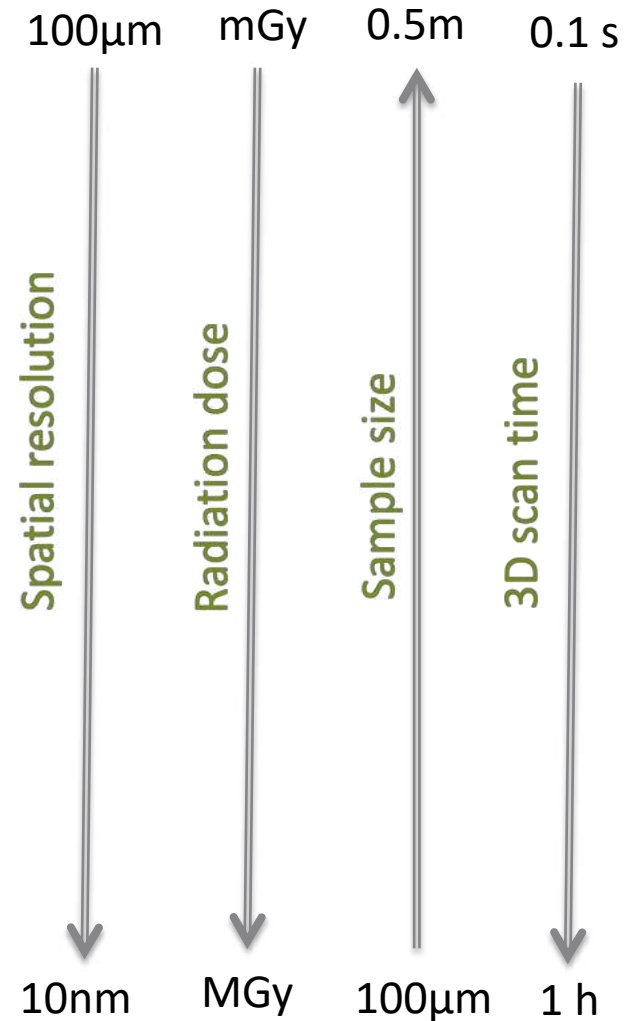
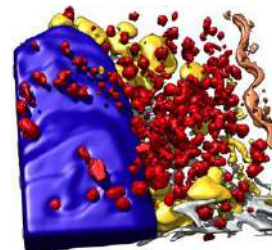
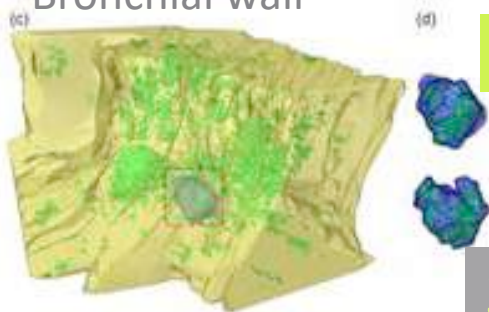


Nano-scale imaging beamlines
(fixed tissue, resolution $\sim 100\text{nm}$, high dose, small samples $\sim 100\ \mu\text{m}$)

Bronchial wall

Fixed tissue

Cell level



3 orders of magnitude in spatial resolution



Aluminum foams

High speed tomography

Al foam – from nucleation to cell wall rupture



Real life system dynamics

*The rise of the Aluminum foam:
From nucleation to film rupture
Acquisition speed: 208 tomo / s
TOMCAT beamline, SLS*

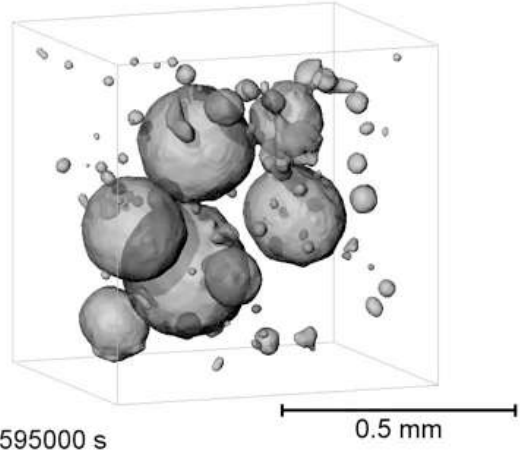
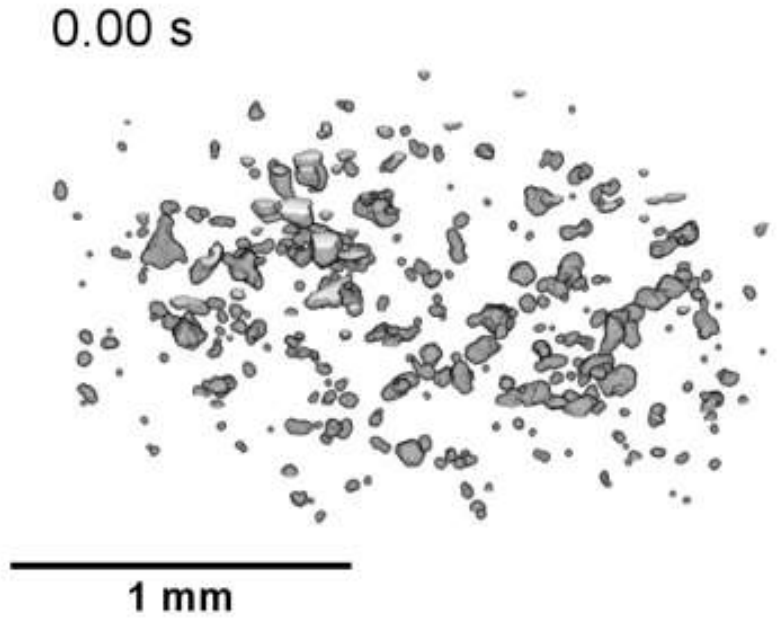
ARTICLE

<https://doi.org/10.1038/s41467-019-11521-1>

OPEN

Using X-ray tomography to explore the dynamics of foaming metal

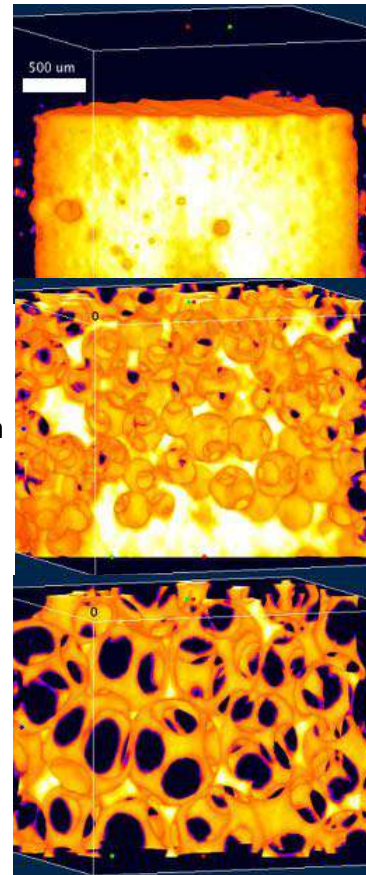
Francisco García-Moreno^{1,2}, Paul Hans Kamm^{1,2}, Tillmann Robert Neu^{1,2}, Felix Bülk^{1,2}, Rajmund Mokso³, Christian Matthias Schlepütz⁴, Marco Stampanoni^{4,5} & John Banhart^{1,2}



PU foams



Nucleation
↓
"Liquid" foam
↓
Solid foam

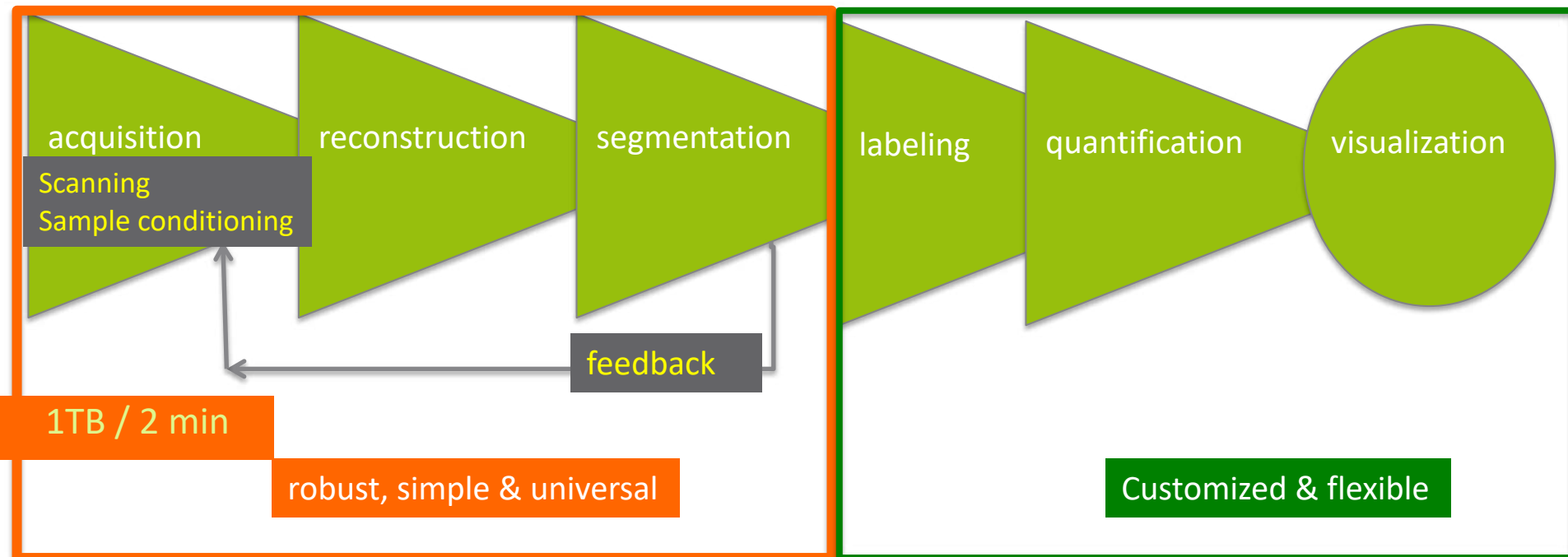
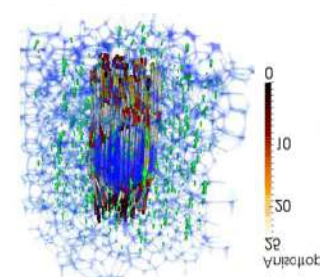
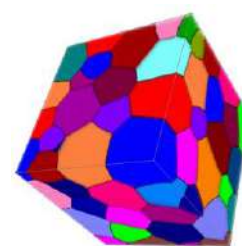
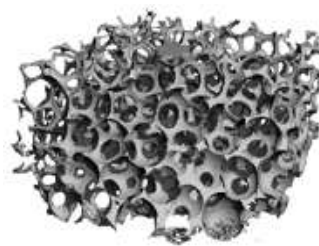
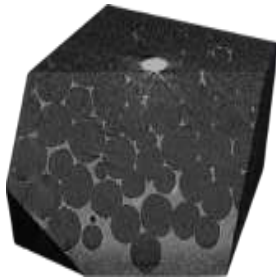
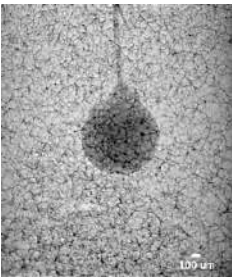


E. Solorzano, S. Alonso, Uni. Valladolid

0.0 sec

Data courtesy of E. Solorzano and S. Alonso, Uni. Valladolid

Image-based quantitative information retrieval

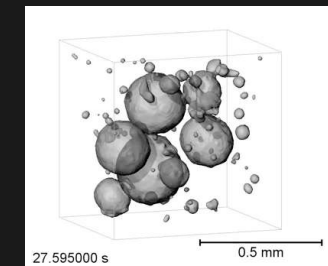
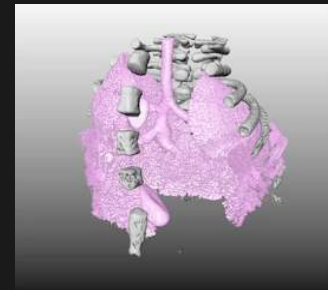
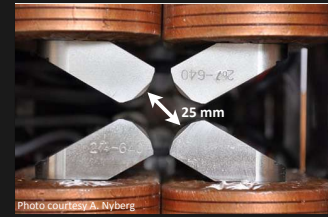


Outline

- I. Brief introduction into tomographic microscopy
 - I. Acquisition and reconstruction

- II. Applications
 - I. Bio: lungs
 - II. Hard matter: Aluminum foams

- III. Overview of MAX IV instruments for imaging
 - I. Beamlines, techniques

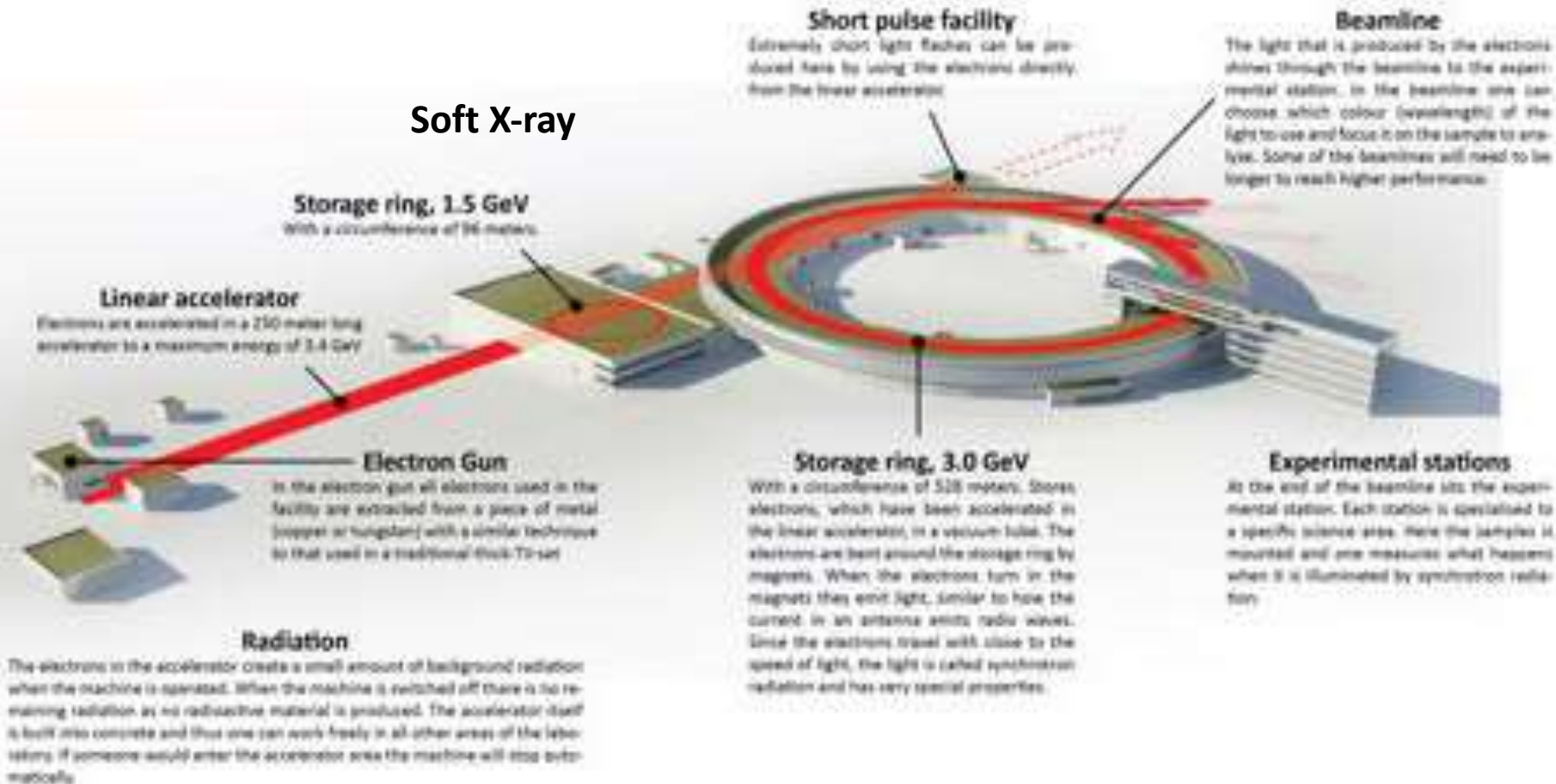




MAX IV

Investment in accelerator ~1150 MSEK
13 initial beamlines ~900 MSEK
+ 3 beamlines

Soft X-ray



MAX IV storage ring

- 528 m circumference, 500 mA with top-up, 20 achromats

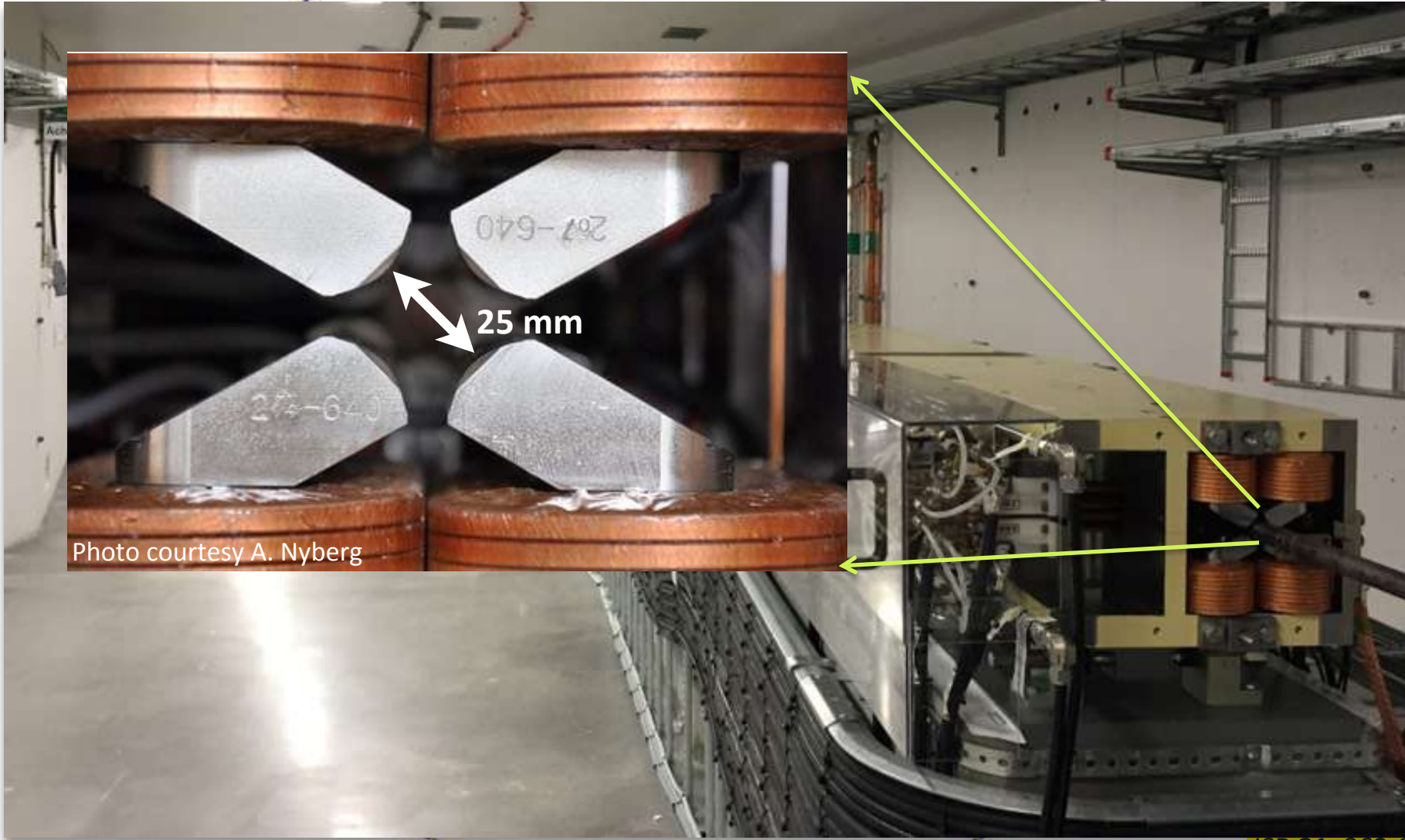


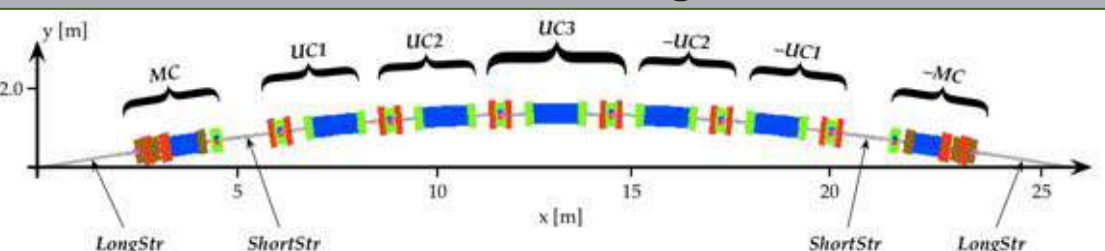
Photo courtesy A. Nyberg

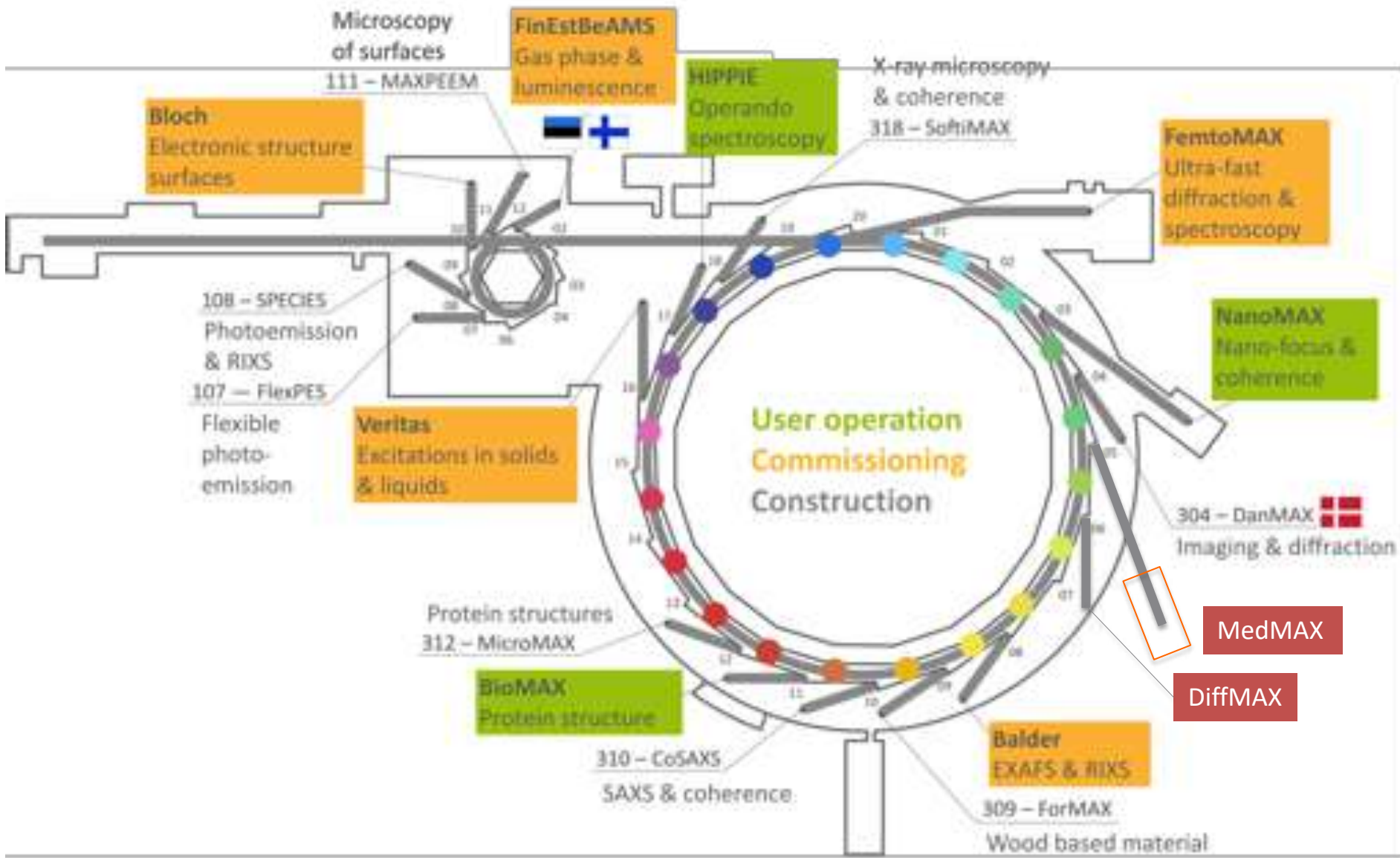
MAX IV magnets

- 528 m circumference, 500 mA with top-up, 20 achromats
- 19 long straights (4.6 m) for users, 1 for injection
- 40 short straights (1.3 m) for RF & diagnostics
- 7-bend achromat: 5 unit cells (3°) & 2 matching cells (1.5° LGB)
- 328 pm rad bare lattice emittance (ϵ_y adjusted to 2-8 pm rad)

Each cell is realized as one mechanical unit containing all magnet elements.

Each unit consists of a bottom and a top yoke half, machined out of one solid iron block, 2.3-3.4 m long.





Tomography in Lund



Zeiss Xradia XRM 520 since 2015
www.solid.lth.se/resources/4d-imaging-lab/

NanoMAX

The nanofocus beamline
(tomography maybe after 2020)

DanMAX

Diffraction & tomography

ForMAX

SAXS beamline with
some tomography

2016

2017

2018

2019

2020

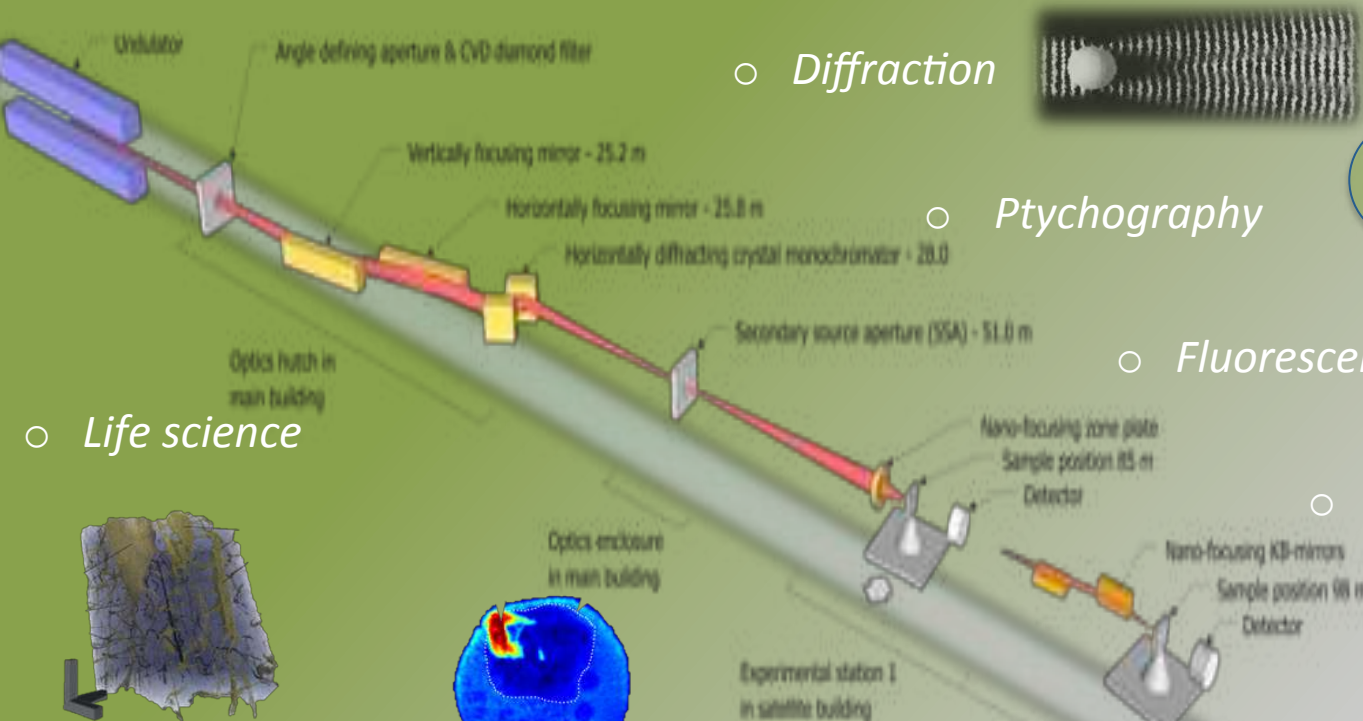
2021

2022

2023

NanoMAX: scanning X-ray nano-probe

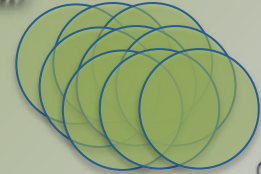
2D & 3D
Structure & strain
Elemental distribution
Morphology



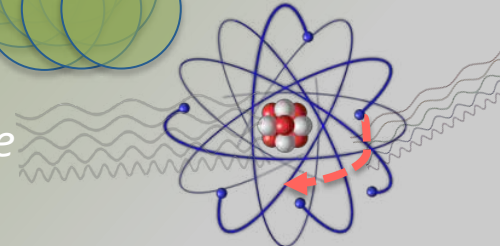
○ Diffraction



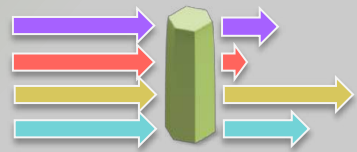
○ Ptychography



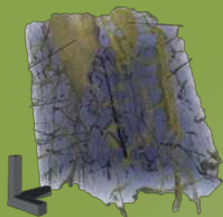
○ Fluorescence



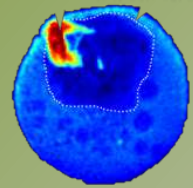
○ Absorption



○ Life science



Bone inner structure by Ptychography
 M Dierolf et al. Nature 2010 467, 436-439



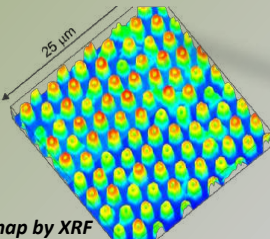
Malaria pigment in red blood cell by XRF
 F. Dubasr et al. Chem. Commun 2012 48, 910

Focusing beam to ~40 nm (10 nm)
Clean and with high degree of coherence

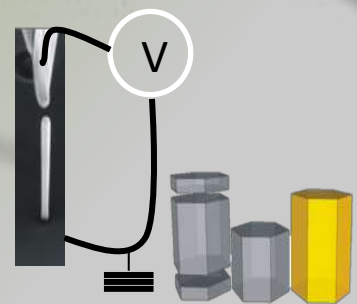
○ Materials science



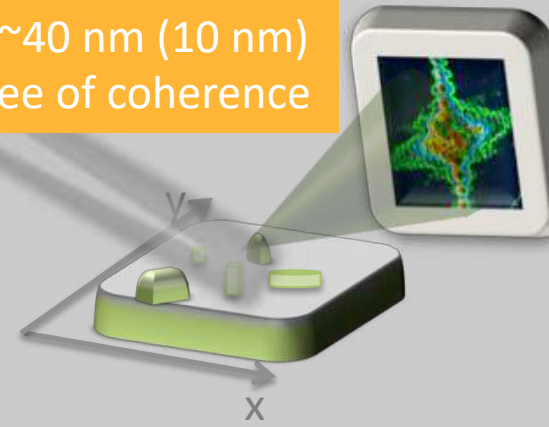
Strain in SiGe device by Bragg ptychography
 S. O. Hruszkewycz et al. arXiv:1506.01262v1
 [cond-mat.mtrl-sci]



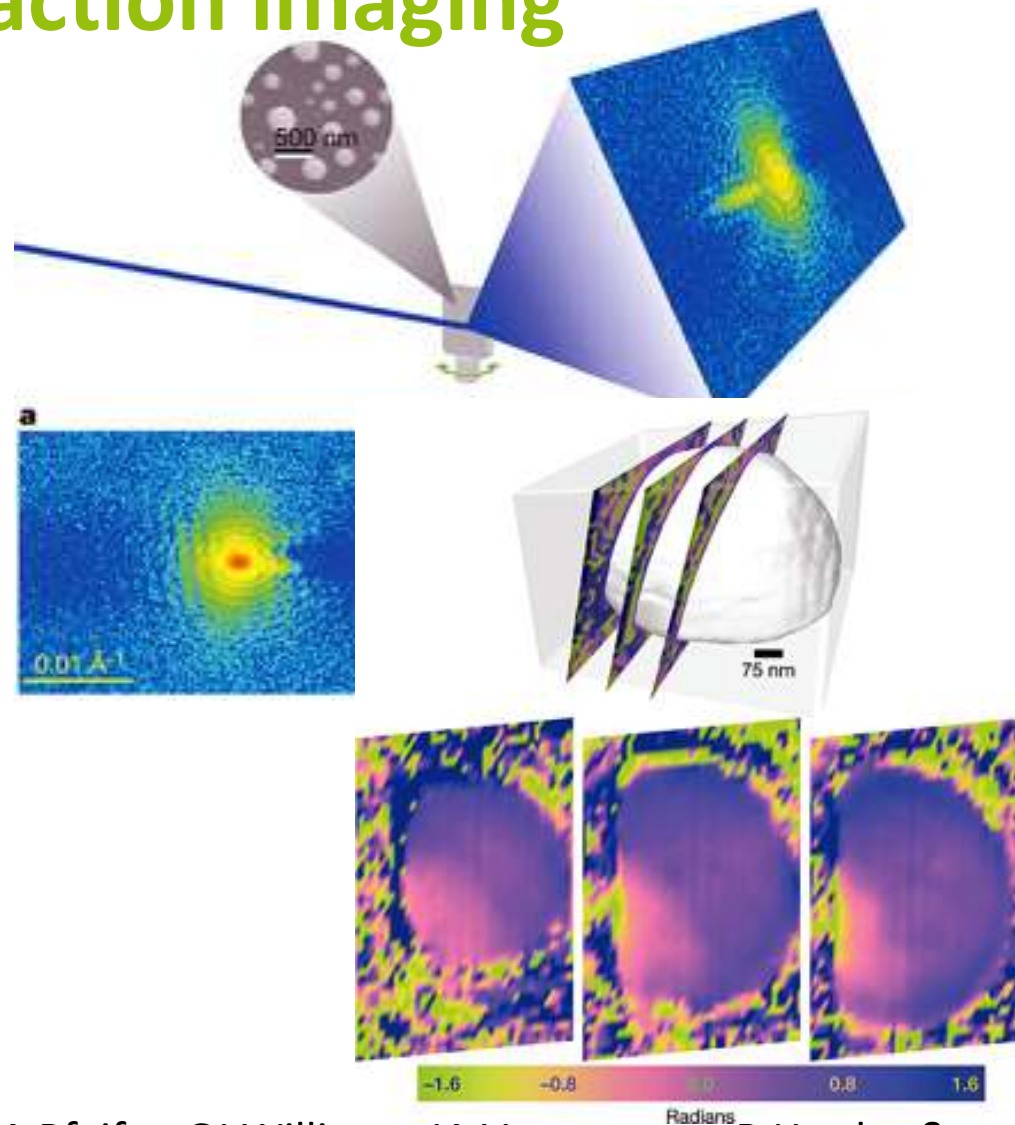
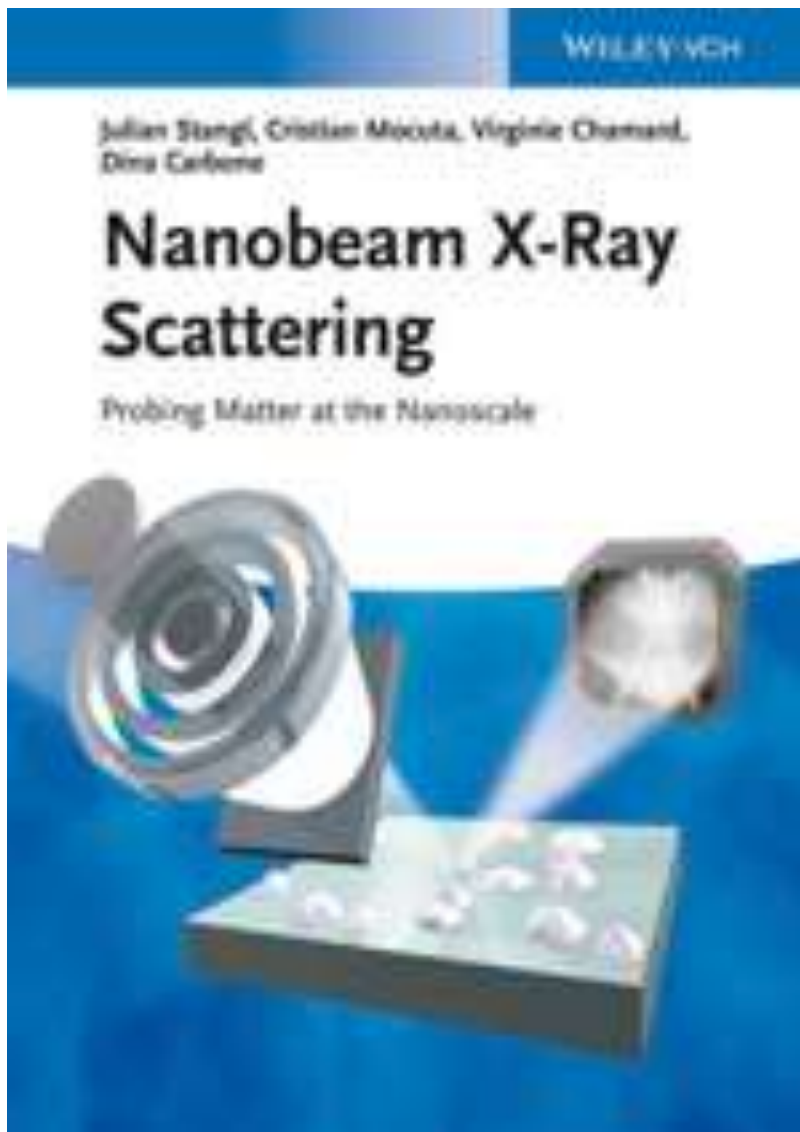
Ga density map by XRF
 G. Martinez-Criado et al
 Nano Lett. (2012) 12, 5829



Structure and transport in GaAs by In-Situ XRD
 G. Bussone et al. Nano Lett. 2015, 15 981



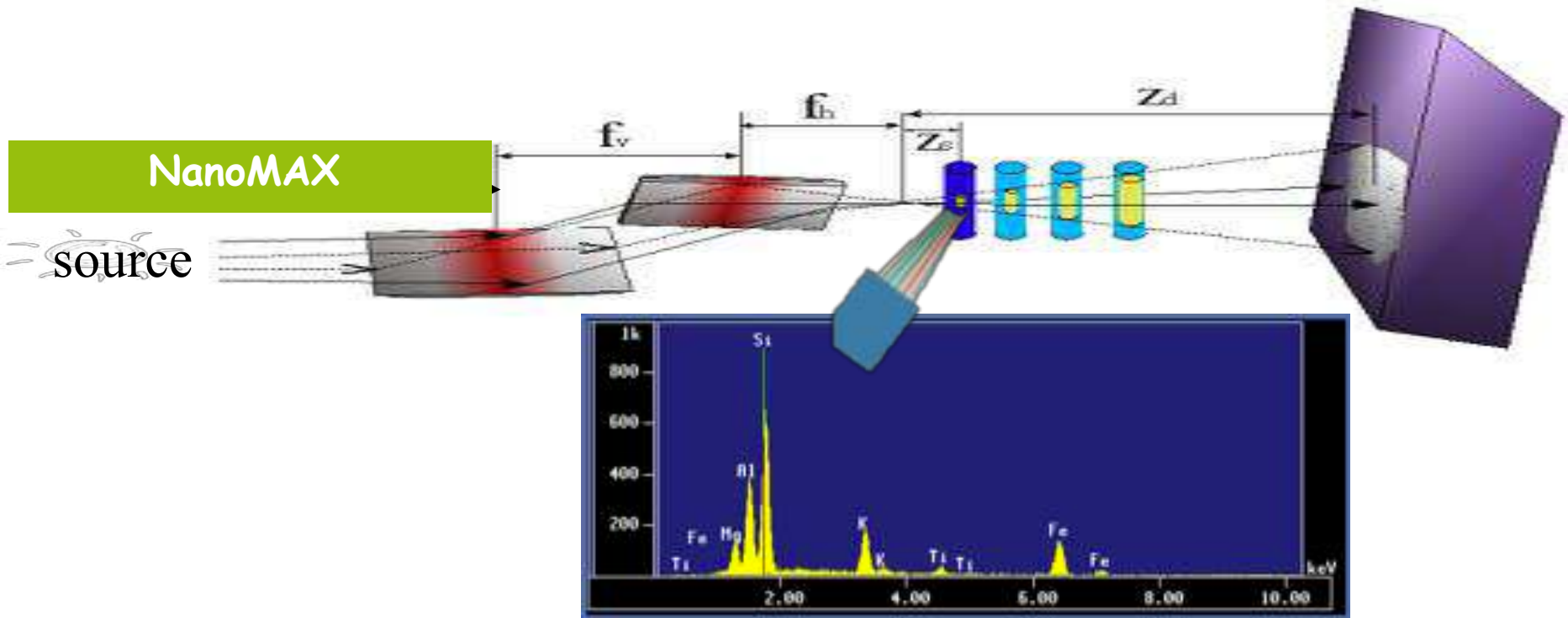
Bragg coherent diffraction imaging



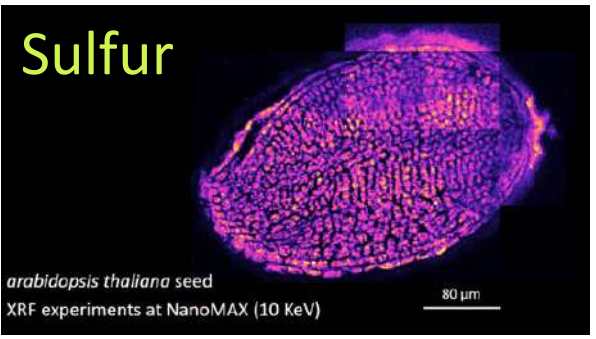
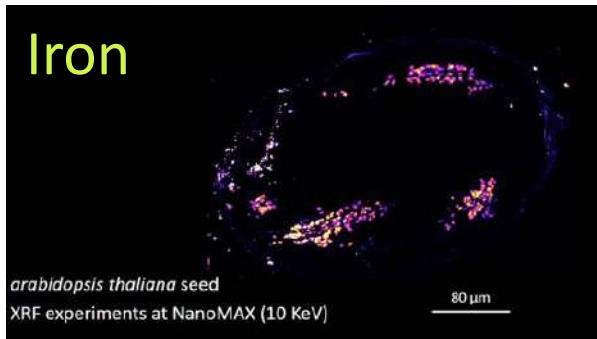
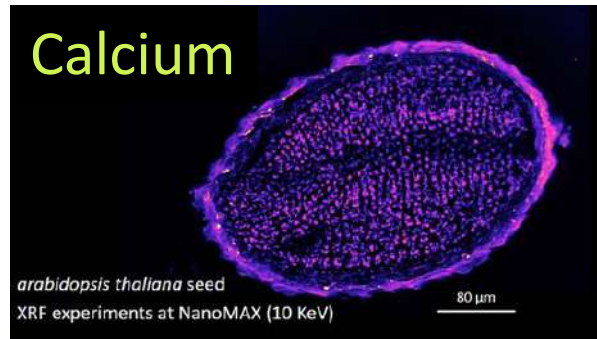
MA Pfeifer, GJ Williams, IA Vartanyants, R Harder & IK Robinson, *Three dimensional mapping of a deformation field inside a nanocrystal.*

Nature 442, 63-66 (2006)

Nanoimaging, Fluorescence spectroscopy



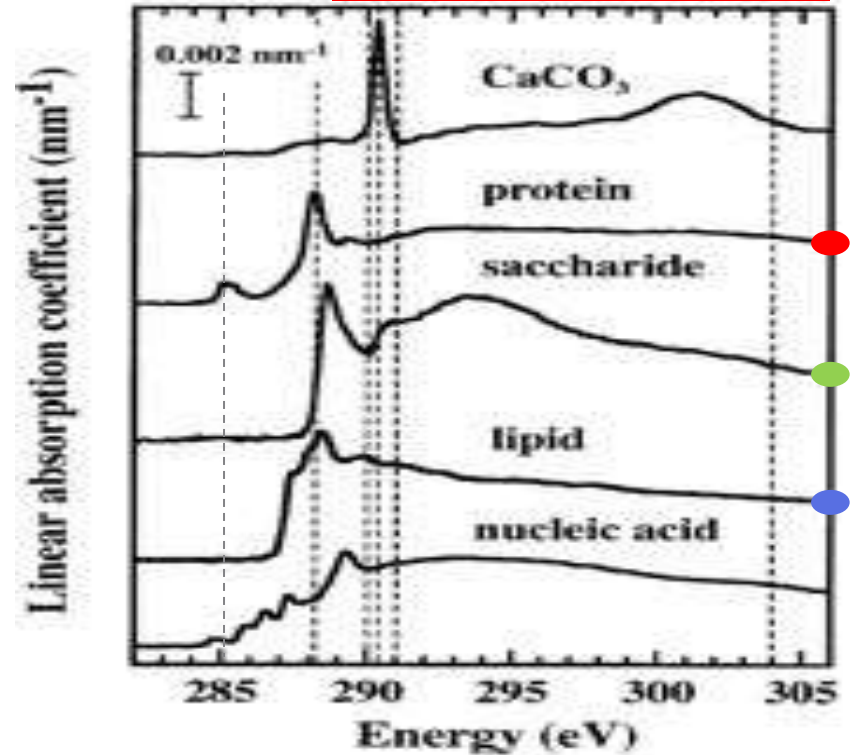
Elemental map distribution in arabidopsis seed



SoftiMAX: Soft X-ray scanning spectro-microscopy

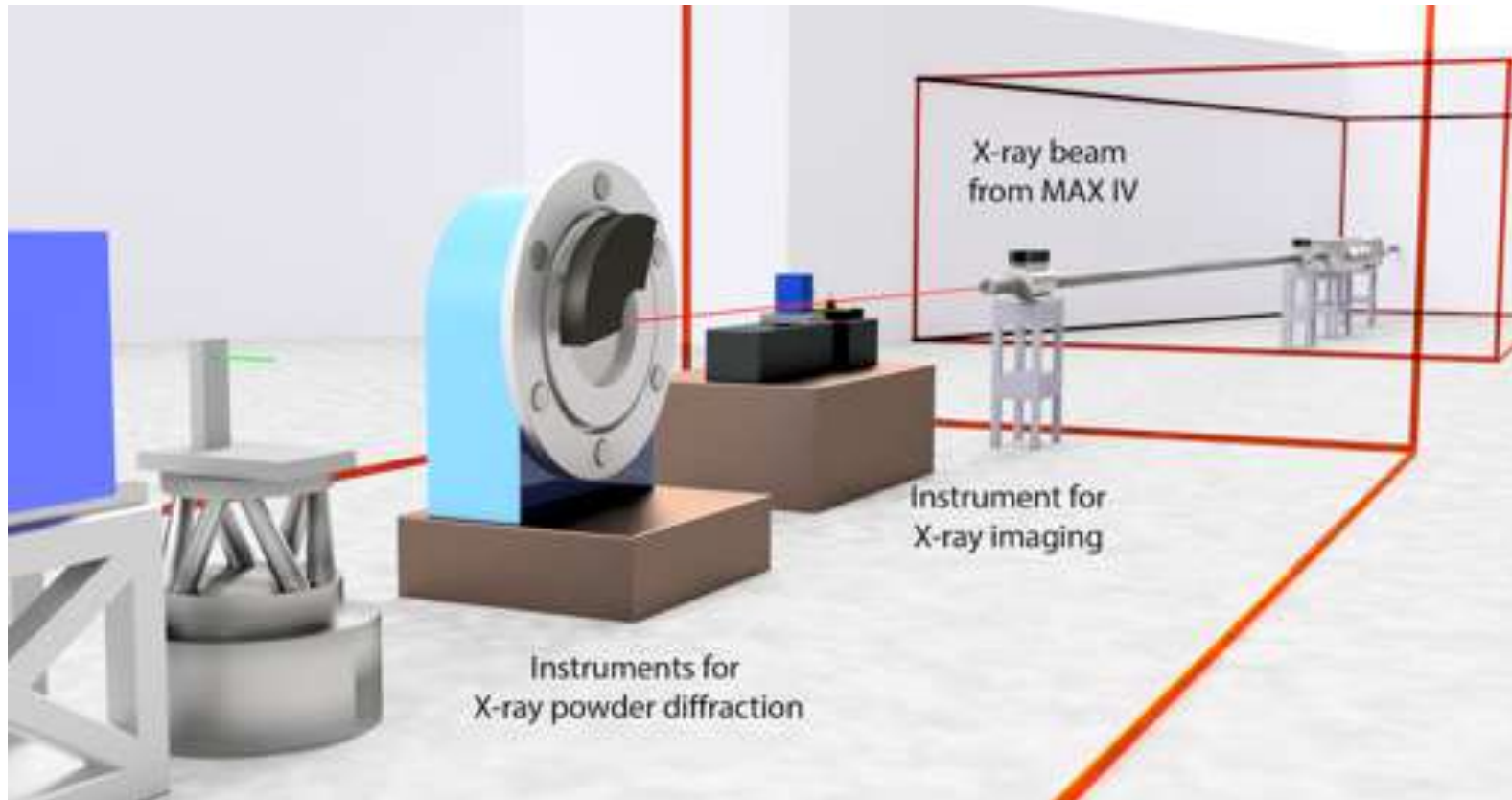


In operation from 2020



Chemical contrast at the nanoscale

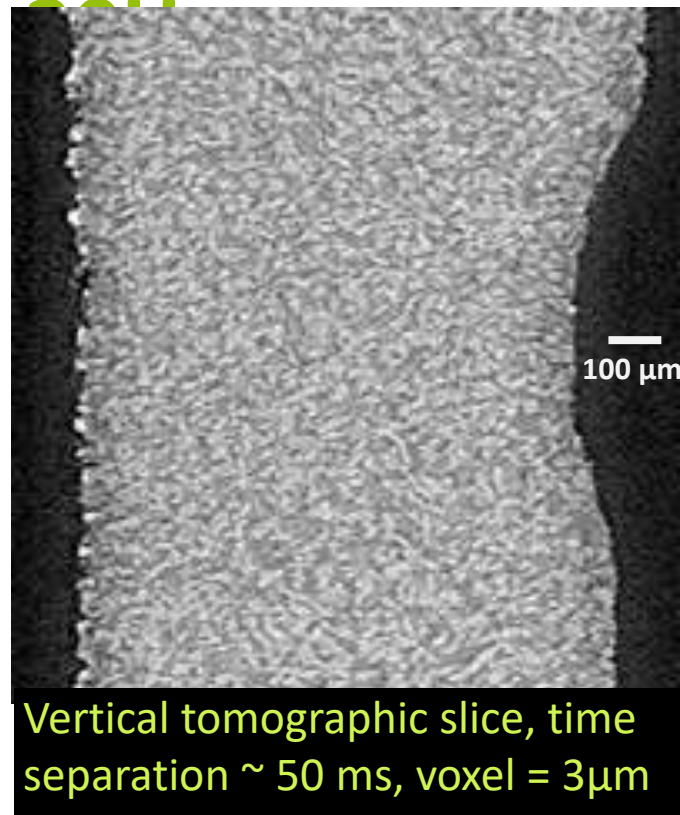
DanMAX: Tomographic microscopy and Powder diffraction



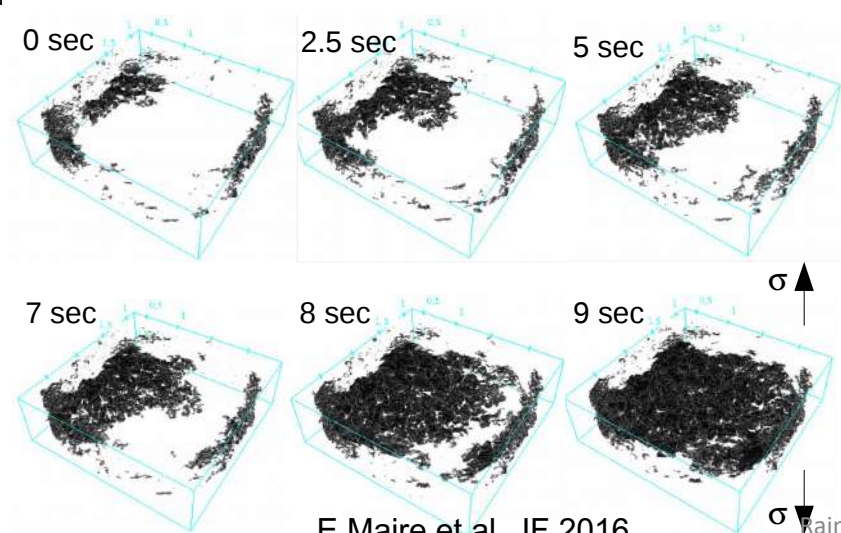
Fast tomography to study in situ materials



Experimental setup @ TOMCAT, Swiss Light Source



Vertical tomographic slice, time separation ~ 50 ms, voxel = 3µm



Al – Alumina (Eric Maire, INSA Lyon)

E.Maire et al. JF 2016

kajmund.Mokso@maxiv.lu.se

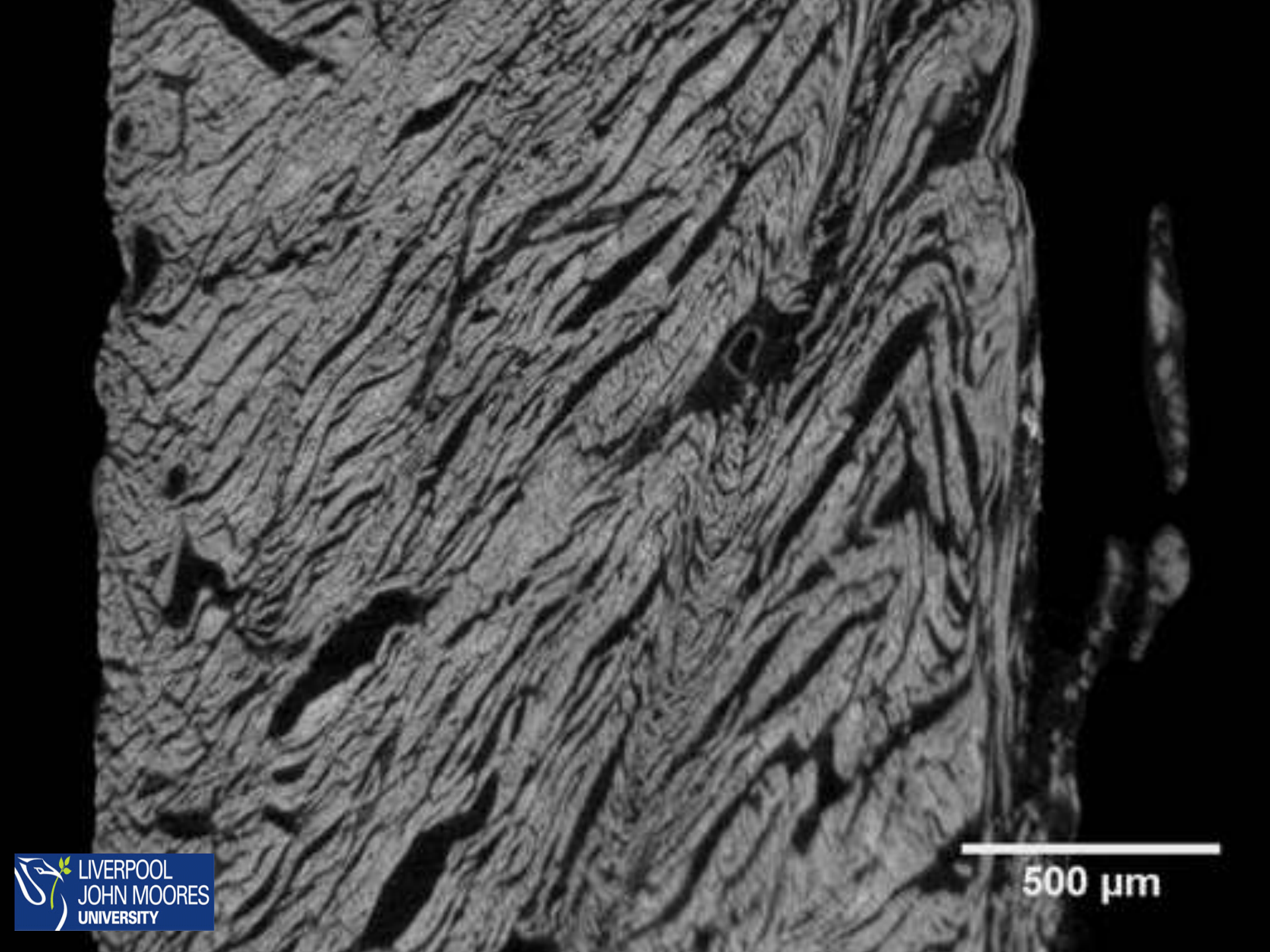
4D IMAGING LAB@LTH

@Division of Solid Mechanics, LTH, Lund

- Installed June 2014 through infrastructure and strategic funding from LTH
- Zeiss Xradia XRM 520 x-ray tomograph
- 3D imaging of bulk objects with resolutions down to < 700 nm
- Focus on “in-situ” and “in-operandi” experiments for “4D imaging”
- Development of software for 3D/4D image analysis and quantification

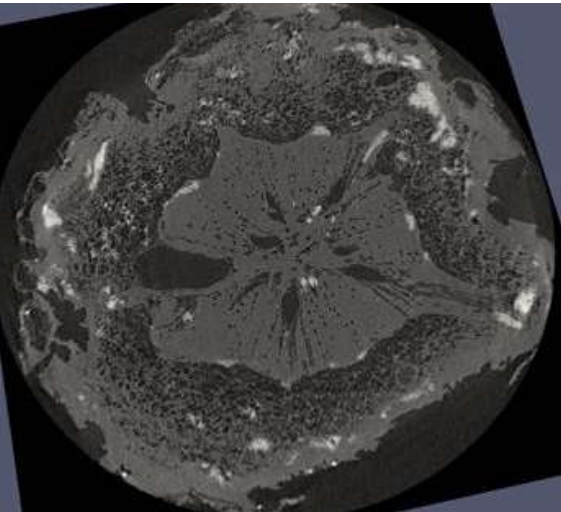
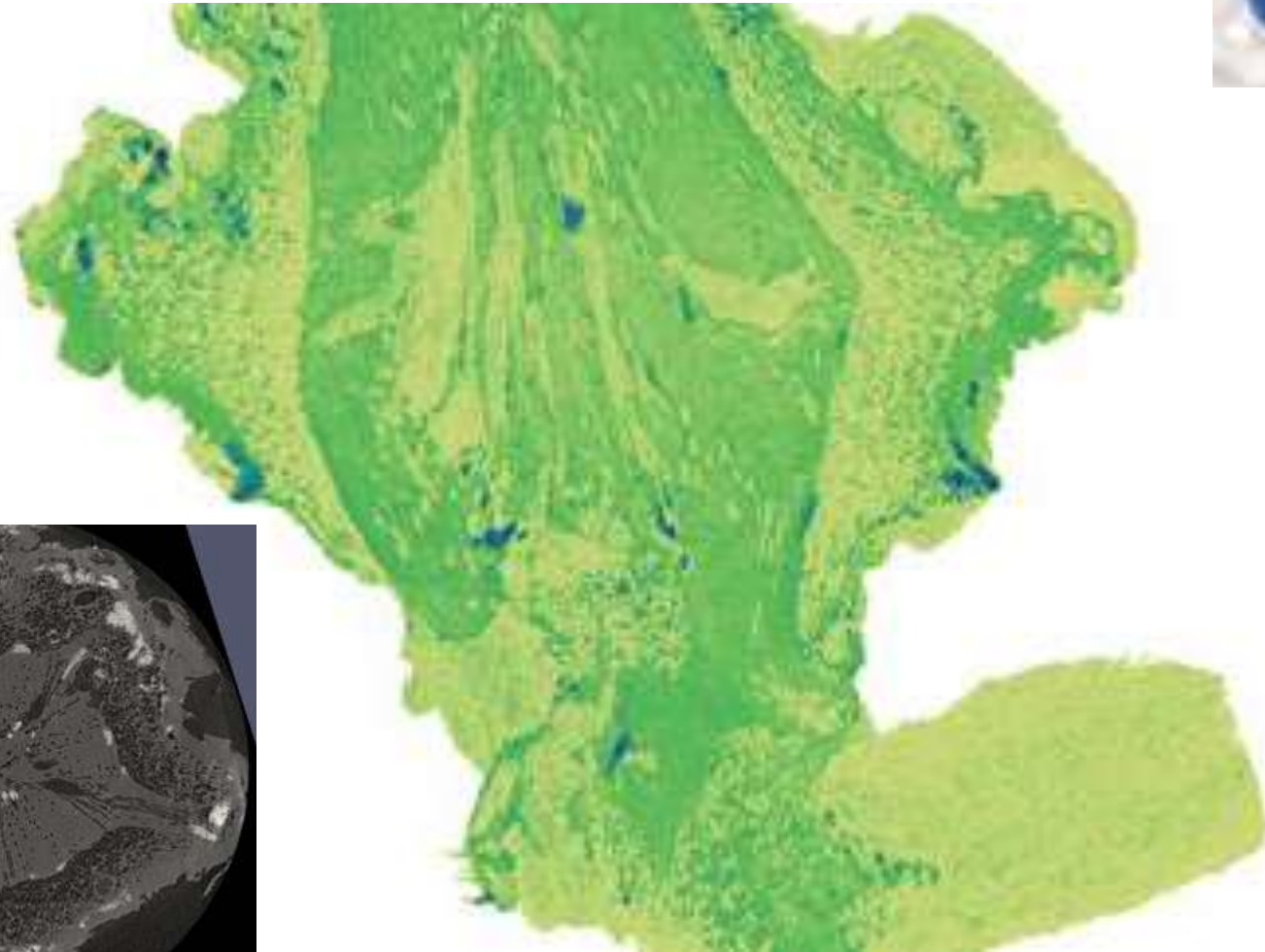
www.solid.lth.se/resources/4d-imaging-lab/





500 μm

Lab CT of grape stem



4D imaging Lab in Lund – Zeiss versa 520, 5 μm spatial resolution in 3D

Conclusions

For tomographic reconstruction we use both numerical and analytical tools. Numerical are still slower.

Synchrotron and lab-based tomographic instruments routinely go down to about $1 \mu\text{m}$ spatial resolution. There is a factor of ~ 100 in acquisition speed between synchrotron and lab-based tomography

In Lund we can do 3D imaging with in 4Dlab (LTH), in a couple of years also at MAX IV